isome proliferator-activated receptor γ (PPARγ), which is expressed at high levels in adipocytes, forms a heterodimeric DNA-binding complex with retinoid X receptor, and acts as a transcriptional regulator of genes involved in adipocyte lipid metabolism. One such reagent, troglitazone, was reported to reduce the excessive islet triglyceride (TG) content of Zucker diabetic fatty (ZDF fa/fa) rats, which led to the restoration of β-cell function and the prevention of lipoapoptosis of β cells.[5,6] Troglitazone has also been shown to reduce TG content in liver and heart of prediabetic ZDF rats[6] or to reduce hepatic TG contents concurrently with improvement of plasma levels of TG and insulin in ZDF fa/fa rats suggesting restoration of SREBP-1 gene expression.[7] To examine effectiveness of thiazolidinediones on the experimental hepatic steatosis caused by chronic ethanol administration, we have herein chosen pioglitazone, another derivative of the antidiabetic reagents; this compound has never been reported so far to cause lactic acidosis or to increase transaminases, whereas troglitazone was withdrawn from the market after a case report of severe hepatic failure.[8] Our attempt to examine the hypothesis in this study has not only shown the effectiveness of pioglitazone but also shed light on significance of the c-Met–mediated signaling pathway to regulate synthesis and removal of triglycerides as a potential therapeutic target for treatment of ethanol-induced hepatic steatosis and injury.

Materials and Methods

Animal Feeding

The Lieber–DeCarli diets were purchased from Bio-Serv, Inc (Frenchtown, NJ).[9] Four-week-old male Sprague–Dawley rats housed in temperature- and light-controlled rooms were randomly divided into 3 groups: (A) rats fed ethanol-containing liquid diet for 6 weeks (n = 9), (B) rats pair fed ethanol-containing liquid diet for 6 weeks during which they were given pioglitazone (10 mg/kg body weight per day) once every 24 hours intragastrically (n = 9), and (C) rats pair fed isocaloric liquid diet without ethanol for 6 weeks (n = 9). Pioglitazone was dissolved in methylcellulose before use. Maeshida et al.[10] reported that pioglitazone was well absorbed from the gastrointestinal tract at an extent of 96% in rats. The plasma concentration of pioglitazone peaked at 4 hours after dosing and declined with a half-life of 2.6 hours. They also showed the concentration of radioactivity in rat tissues at 0.5, 2, 6, 10, 24, and 72 hours after oral administration of [^{14}C]pioglitazone.[10] The radioactivity of liver tissue was higher than that of plasma, and it peaked at 6 hours. The concentration of pioglitazone in liver at 24 hours after oral administration is still about one third of the concentration at 30 minutes. There is another report describing that 1 dose of 10 mg/kg of pioglitazone every 24 hours ameliorated insulin resistance associated with diabetes in rats.[11] Based on these previous papers, we think it reasonable to expect that 1 dose of 10 mg/kg of pioglitazone every 24 hours is sufficient to sustain effective concentration. The rats in groups A and C were given methylcellulose once every 24 hours intragastrically for 6 weeks in the same amount as their corresponding litter mates in group B. The rats in group B and group C were pair fed daily on an isoenergetic basis with the corresponding litter mates fed the ethanol-containing diet (group A). To investigate whether another thiazolidinedione, troglitazone, could prevent alcoholic fatty liver, we next gave troglitazone (200 mg/kg body weight/day) to 8-week-old male SD rats (n = 6), instead of pioglitazone, in the same way as our last examination of pioglitazone. Troglitazone was also well absorbed from the gastrointestinal tract, and the highest uptake by the liver was shown in rats.[12] All animals received humane care in compliance with the National Research Council's criteria outlined in the "Guide for the Care and Use of Laboratory Animals" prepared by the U.S. National Academy of Sciences and published by the U.S. National Institutes of Health.

Biochemical and Histological Analysis

Hepatic triglyceride contents were measured as previously described.[13] For histological analysis, liver tissue was fixed in 4% paraformaldehyde and embedded in paraffin. Alternatively, hepatic lipids were stained by an oil red O method (Nacalai Tesque Inc., Kyoto, Japan). For protein or RNA analysis, tissue was frozen in liquid nitrogen and stored at −80°C until used. Apoptosis was analyzed with TUNEL staining (Apoptosis Detection System, Promega Corp., Madison, WI) according to the manufacturer's instructions. At least 2 individual livers were examined in each group by counting the density of the positive-staining hepatocytes in 5 random × 200 fields/liver. Serum concentrations of alanine aminotransferase (ALT), aspartate aminotransferase (AST), triglyceride, total cholesterol, phospholipids, total proteins, albumin, and free fatty acids were measured with a standard clinical autoanalyzer (Hitachi 7170; Hitachi Ltd., Tokyo, Japan). Plasma glucose was measured by the glucose oxidase method with a glucose analyzer II (Beckman Instruments, Brea, CA). Plasma TG levels were measured with a GPO-Trinder triglyceride kit (Sigma, St. Louis, MO). Plasma leptin and insulin were assayed with Linco leptin and insulin assay kits (Linco Research Immunoassay, St. Charles, MO). Serum low-density lipoprotein cholesterol was measured by the direct enzymatic method[14] with Cholestest LDL (Daiichi Pure Chemicals Co., Ltd, Tokyo, Japan). Serum very low–density lipoprotein (VLDL) cholesterol was separated by a modification of the method of Hatch and Lees.[15] A commercially available enzyme-linked immunosorbent assay kit was used to determine serum tumor necrosis factor-α (TNF-α).

Table 1. Primer and Taqman Probe Sequences for Real-Time PCR

Gene	Sense primer (5′-3′)	Antisense primer (5′-3′)	Taqman probe (5′-3′)
c-Met	5′-CGACATTCAGTCCGAGGTTCA-3′	5′-GGGACACTGGCCTGACTCTTC-3′	5′-TGCATGTTCTCCCCACTTGCGG-3′
HGF	5′-GACATGTCTTGCCTGATTCTGTGT-3′	5′-AGTCTGTGACATTCCTCAGTGTTCA-3′	5′-TCACCGTTGCAGGTCATGCATTCA-3′
HOX1	5′-CACCTTCCCGAGCATCGA-3′	5′-AGGCGGTCTTAGCCTCTTCTGT-3′	5′-CTCGCATGAACACTCTGGAGATGACC-3′
MT1	5′-CTGCTCCACCGGCGG-3′	5′-GCCCTGGGCACATTTGG-3′	5′-CTCCTGCAAGAAGAGCTGCTGCTCCT-3′
MT2	5′-TCCTGTGCCACAGATGGATC-3′	5′-GTCCGAAGCCTCTTTGCAGA-3′	5′-AAAGCTGCTGTTCCTGCTGCCCC-3′
SREBP1a	5′-ACACAGCGGTTTTGAACGACA-3′	5′-GCATCAAATAGGCCAGGGAA-3′	5′-CATGCTTCAGCTCATCAACAACCAAG-3′
SREBP1c	5′-GGAGCCATGGATTGCACATT-3′	5′-GCATCAAATAGGCCAGGGAA-3′	5′-CATGCTTCAGCTCATCAACAACCAAG-3′
SCD1	5′-CCTCATCATTGCCAACACCAT-3′	5′-AGCCAACCCACGTGAGAGAA-3′	5′-TTCTCTGAGACACACGCCGACCCTC-3′
SCD2	5′-ACCGCTGGCACATCAACTTC-3′	5′-GGACACCCTCTTCCGGTCAT-3′	5′-CCACGTTCTTCATCGACTGCATGGC-3′

Real-Time Quantitative PCR Analysis

Total RNA was extracted from the liver with ISOGEN (Nippon Gene, Tokyo, Japan) according to the method of Chomczynski and Sacchi, as previously described.[16] For the reverse-transcriptase reaction, TaqMan reverse transcription reagents (Applied Biosystems, Foster City, CA) were used. Briefly, the reverse-transcriptase reaction (final volume of 50 μL) was conducted for 60 minutes at 37°C followed by 25°C for 10 minutes using random hexamers. Polymerase chain reaction (PCR) amplification was performed with TaqMan Universal Master Mix (Applied Biosystems). In brief, reactions were performed in duplicate containing 2× Universal PCR master mix, 2 μL of template cDNA, 900 nmol/L of primers, and 250 nmol/L of probe in a final volume of 50 μL and were analyzed in a 96-well optical reaction plate (Applied Biosystems). Primers and probes were synthesized by Applied Biosystems custom oligo synthesis service. Sequences of primers and probes are shown in Table 1. Probes include a fluorescent reporter dye, FAM, on the 5′ end and labeled with fluorescent quencher dye, TAMRA, on the 3′ end to allow direct detection of the PCR product. Reactions were amplified and quantified using an ABI 7700 sequence detector and manufacturer's software (Applied Biosystems). The threshold cycle (Ct) indicates the fractional cycle number at which the amount of amplified target reaches a fixed threshold. The relative quantity of target messenger RNA (mRNA) was obtained using the comparative Ct method and was normalized using predeveloped TaqMan assay reagent rat 18S ribosomal RNA as an endogenous control (Applied Biosystems) (for details, see user Bulletin 2 for the ABI PRISM 7700 Sequence Detection System under www.appliedbiosystems.com/support/tutorials). Briefly, the TaqMan software (Applied Biosystem) was used to calculate a Ct value for each reaction, where the Ct value is the point in the extension phase of the PCR reaction that the product is distinguishable from the background. The Ct values were then normalized for amplification by subtracting the Ct value calculated for 18S ribosomal RNA, an endogenous control for the amount of mRNA from the same sample, to obtain a Ct using the following equation: Ct target − Ct 18S ribosomal RNA = Ct. The fold induction was calculated relative to the Ct value obtained in the control rats or cells. The normalized expression was calculated as fold changes in a quantity of mRNA. TNF-α mRNA was measured using predeveloped TaqMan assay reagent rat TNF-α (Applied Biosystems) (for details, see user Bulletin 2 for the ABI PRISM 7700 Sequence Detection System under www.appliedbiosystems.com/support/tutorials).

Isolation and Primary Culture of Rat Hepatocytes

Primary cultured hepatocytes were prepared from livers of ethanol-fed rats through a collagenase perfusion method in group A as described elsewhere.[17] The isolated hepatocytes were cultured on gelled pig tendon collagen (Cellmatrix, Nitta zerachin, Ltd., Osaka, Japan), and the second layer of collagen gel was spread over the cells after 1 day of incubation as previously described.[17] A PPARγ-selective agonist AD4833 (pioglitazone hydrochloride, Takeda, Ltd., Osaka, Japan)[18] and troglitazone (Sankyo, Ltd., Tokyo, Japan)[5] was dissolved in dimethyl sulfoxide (DMSO) and added to the hepatocytes at various doses in a volume at 0.05% of the medium. In the control, the medium was supplemented with the same volume of DMSO.

Transcriptome Analyses by DNA Microarray

Transcriptome analyses were performed by using DNA microarrays (Atlas cDNA expression arrays, Clontech). Preparation of ^{33}P-labeled cDNA samples, hybridization, and washing were carried out with total RNA of the liver tissue according to the manufacturer's manual. All data sets were normalized to the signal density of housekeeping genes, such as the gene encoding glyceraldehyde-3-phosphate dehydrogenase, and total radioactivity, which represents the total amount of cDNA hybridized to the microarrays. The threshold for determining the significance of changes in the level of gene expression was established by using an algorithm that requires both a significant absolute and significant fold change.[19,20]

Western and Immunoprecipitation Analysis

Total cellular protein (50 μg) collected from snap-frozen liver was subjected to Western blot analysis for c-Met, mature hepatocyte growth factor (HGF), and apolipoprotein B (apoB)100. For immunoblot analyses, primary antisera were used at the concentration of 1:100. The membranes were

probed with antirat c-Met antibody (Santa Cruz Biotechnology, Santa Cruz, CA), anti-rat HGFα antibody (Santa Cruz Biotech), and anti-rat apoB antibody (Santa Cruz Biotech). For immunoprecipitation, lysates (10 mg of protein) were incubated with protein A-agarose beads (Pierce, Rockford, IL) to precipitate the antigen-antibody complex. Samples were separated by SDS-PAGE on 10% polyacryamide gels. After electrophoresis, the gel was transferred to polyvinylidine difluoride sheets, which were subsequently probed with anti-phosphotyrosine antibody (PY-20; ICN Biomedicals Inc., Aurora, OH) or antirat c-Met antibody. Then, they were incubated with a chemiluminescence substrate (ECL reagent: Amersham Life Science, Buckinghamshire, UK) and exposed to Hyperfilm-MP (Amersham). Densitometric analysis was performed with National Institutes of Health Image Data analysis software.

Immunohistochemistry

For detection of 4-hydroxynonenal (4-HNE) protein adducts, paraffinized sections were deparaffinized, rehydrated, treated with normal horse serum, and incubated with mAb anti-4-HNE (0.625 μg/mL) (Nippon Rouka Seigyo Kenkyuujo, Tokyo, Japan) overnight at 4°C. After several washes with phophate-buffered saline, the sections were stained with biotinylated antimouse IgG for 1 hour (Vectastain Elite ABC kit; Vector Laboratories, Inc., Burlingame, CA). To prevent endogenous peroxidase reactions, the samples were pretreated with 0.3% H_2O_2 in cold methanol for 30 minutes and were subsequently incubated with avidin and horseradish peroxidase (HRP)-conjugated biotin for 30 minutes, followed by detection with 3,3′-diaminobenzidine solution containing 0.003% H_2O_2.

Measurement of DNA Synthesis

DNA synthesis was measured by bromodeoxyuridine (BrdU) incorporation with a Cell Proliferation ELISA, BrdU kit (Roche Molecular Biochemicals, Mannheim, Germany). In brief, hepatocytes were suspended in William's medium E supplemented with 10% fetal bovine serum (FBS), 10 nmol/L insulin, 10 nmol/L dexamethasone, penicillin (5 U/mL), and streptomycin (50 μg/mL) and seeded at a density of 5×10^4 cells/cm^2 on collagen-coated dishes. The culture medium was exchanged after 4 hours for William's medium E supplemented with 10% FBS. After incubation in William's medium E with 10% FBS for approximately 20 hours, the culture medium was exchanged for William's medium E containing 10% FBS with HGF/SF, pioglitazone, or both. They were then cultured for another 24 hours with the addition of BrdU and were harvested in determining the BrdU incorporation into cellular DNA according to the manufacturer's instructions.

Analyses for Effects of Pioglitazone on Ethanol Metabolism in Rats

Four-week-old male Sprague–Dawley rats were randomly divided into 2 groups: rats fed the Lieber–DeCarli control liquid diet for 10 days (n = 16) and those pair fed isocaloric control liquid diet for 10 days during which they were given pioglitazone (10 mg/kg body weight/day) once every 24 hours intragastrically (n = 16). After overnight starvation, rats were given ethanol intragastrically at 4 g/kg body weight on the 10th day. Before and 2, 12, and 24 hours after the ethanol administration, 4 rats in each group were sacrificed to collect heparinized blood samples which were immediately deproteinized to determine ethanol and acetaldehyde concentrations through gas chromatography.[21]

Statistical Analysis

All data are expressed as the mean ± standard error. Statistical analysis was performed by using the unpaired Student *t* test or by 1-way analysis of variance. When the analysis of variance analyses were applied, differences in mean values among groups were examined by Fisher's multiple comparison test.

Results

Pioglitazone Attenuates Hepatic Steatosis Caused by Chronic Ethanol Administration

The hepatic triglyceride concentration in rats given the isocaloric pair fed liquid diet was 9.67 (±4.34) mg/g liver weight, as opposed to 78.24 (±11.25) mg/g liver weight in the rats given the ethanol-containing diet for 6 weeks (Table 2). Histological analysis showed that lipid droplets accumulated in the hepatocytes in pericentral regions but not in those in periportal regions in the ethanol-fed rats. On the other hand, such changes were not notable in the control liver even with the lipid-specific oil red staining (Figure 1). Pioglitazone (10 mg/kg per day) markedly decreased accumulation of lipid droplets in both perivenular and the periportal regions with the total body weight remaining unchanged (Figure 1). In good agreement with these results, hepatic triglyceride levels became as low as in the pair-fed control rats (Table 2). Treatment with methylcellulose as a vehicle had no effect on either triglyceride contents or histology in the liver (data not shown). The ethanol feeding caused an increase in the liver weight/body weight ratio and a decrease in the epididymal fat weight/body weight ratio, whereas pioglitazone treatment prevented these changes (Table 2).

Analyses of serum AST and ALT activity to assess the effect of pioglitazone on liver function showed that pioglitazone suppressed the elevation of serum concentrations of AST and ALT in ethanol-fed rats (Table 2), and this improvement was associated with improvement in histological findings in the liver. Ethanol feeding caused elevations of the serum concentrations of free fatty acids,

Table 2. Body Weight and Serum Biochemical Parameters in the Treated Groups

	Ethanol (n = 8)	Ethanol + Pioglitazone (n = 8)	Control (n = 8)
Liver weight/body weight (%)	[b]3.57 (0.34)	3.08 (0.24)	2.35 (0.25)
Epididymal fat weight/body weight (%)	[a]0.574 (0.044)	0.808 (0.065)	0.806 (0.062)
Liver triglyceride (mg/g liver weight)	[a]78.24 (11.25)	14.36 (3.72)	9.67 (4.34)
AST (IU/L)	[a]362.4 (25.4)	195.7 (23.3)	38.1 (10.6)
ALT (IU/L)	[a]174.2 (13.4)	50.3 (4.9)	33.5 (5.2)
Phospholipid (mg/dL)	159.2 (10.8)	146.7 (14.2)	110.0 (7.3)
FFA (mEQ/L)	0.562 (0.126)	0.550 (0.240)	[a]0.448 (0.066)
Total cholesterol (mg/dL)	116.0 (8.9)	130.8 (20.9)	[a]72.7 (7.1)
LDL (mg/dL)	82.4 (15.8)	98.0 (22.3)	45.4 (7.9)
VLDL (mg/dL)	7.25 (0.23)	7.96 (0.35)	6.94 (0.28)
Triglyceride (mg/dL)	21.67 (3.68)	20.35 (2.76)	[a]14.58 (2.64)
Leptin (ng/mL)	0.62 (0.25)	1.55 (1.25)	0.82 (0.46)
TNF-α (pg/mL)	22.26 (4.48)	23.32 (3.87)	25.02 (4.87)

NOTE. Results (and standard error of the mean) from 8 rats/group at the end of feeding period.
[a]$P < 0.05$ versus both other groups.
[b]$P < 0.05$ versus the control group.

triglyceride, phospholipid, total cholesterol, and LDL, and pioglitazone caused elevation of serum VLDL levels, but no significant changes were found in serum TNF-α or leptin levels (Table 2). We did not find any significant changes in total protein, albumin, glucose, insulin, lactic acid, or choline esterase levels (data not shown).

Transcriptome Analyses for Mining Genes Responsible for Antisteatotic Effects of Pioglitazone

To elucidate mechanisms by which pioglitazone reduces hepatic lipid contents in alcoholic fatty liver, we

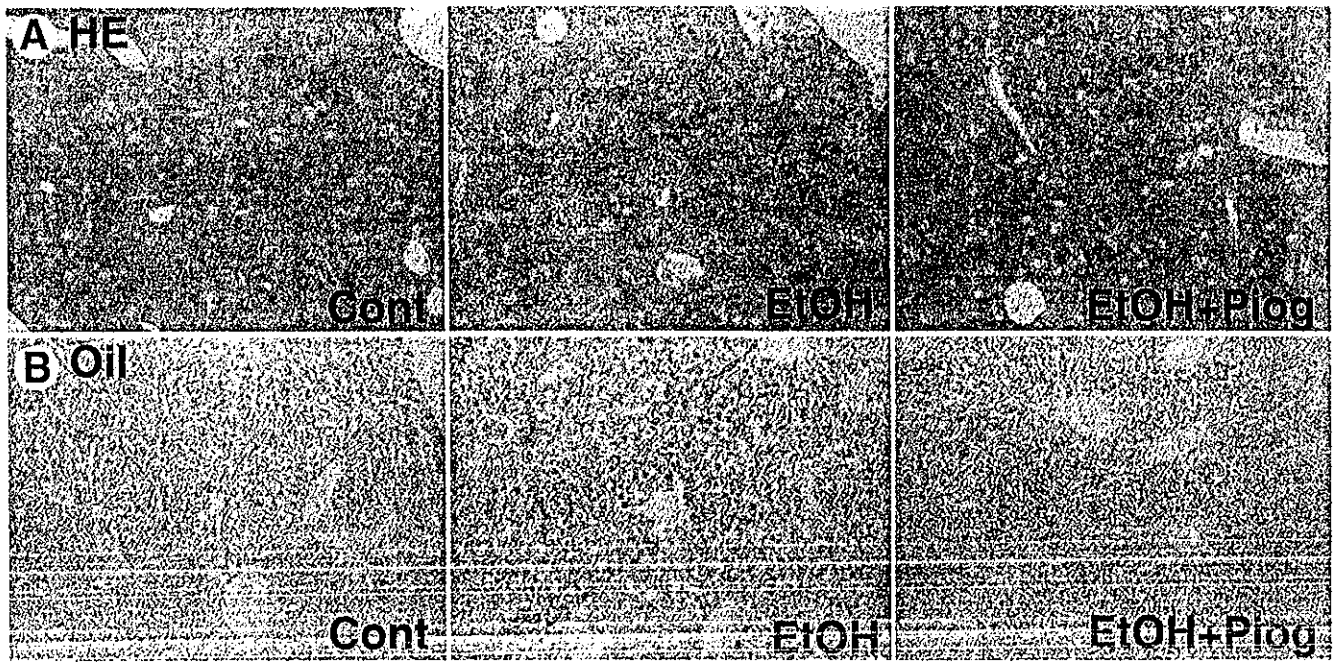

Figure 1. Effect of pioglitazone on liver histology in the ethanol-fed rats. (*A*) H&E-stained sections of representative liver samples of control rats (Cont), ethanol-fed rats (EtOH), and ethanol-fed rats given pioglitazone (EtOH+Piog) (×40). Minimal steatosis or no change was seen in the livers of the pair-fed control rats. Severe macrovesicular steatosis was observed preferentially in the perivenular areas in the ethanol-fed rats. Pioglitazone markedly decreased accumulation of lipid droplets in both the perivenular and the periportal areas. Only minimal steatosis was left in the livers of ethanol-fed rats given pioglitazone. (*B*) Oil red–stained sections of representative liver samples of control rats, ethanol-fed rats, and ethanol-fed rats given pioglitazone (×40). Specific staining of lipid accumulation was shown. Pioglitazone markedly decreased accumulation of lipid droplets.

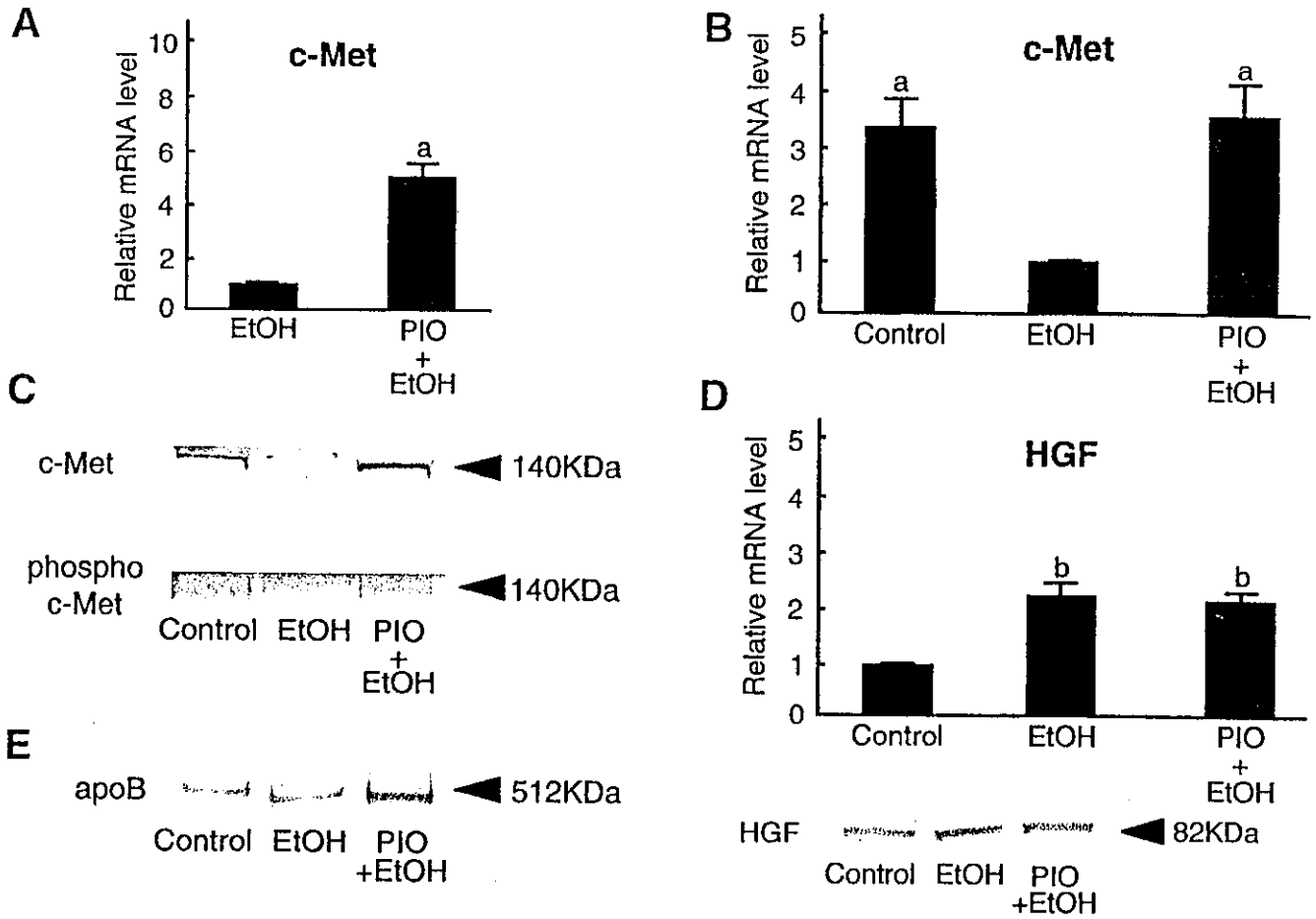

Figure 2. Hepatic c-Met, HGF, and apoB expression. (*A*) DNA microarray analysis showed that pioglitazone increased hepatic c-Met mRNA expression. Results (and standard error of the mean) from 3 rats/group at the end of feeding period. $^{a}P < 0.05$ versus the ethanol-fed group. EtOH, ethanol-fed rats; PIO+EtOH, ethanol-fed rats given pioglitazone. (*B*) Real-time PCR analysis showed that chronic ethanol feeding decreased hepatic c-Met expression and that pioglitazone prevented this decrease. Results (and standard error of the mean) from 6 rats/group at the end of feeding period. All real-time quantitative PCR reactions were carried out in duplicate. $^{a}P < 0.05$ versus the ethanol-fed group. (*C*) Western immunoblot analysis of expression of c-Met (*upper*) and tyrosine phosphorylation of c-Met (*lower*) in liver homogenates (containing 50 μg of total protein each). (*D*) Real-time PCR analysis (*upper*) and Western blotting analysis (*lower*) showed that chronic ethanol feeding increased hepatic HGF expression and pioglitazone had no effect on this. Results (and standard error of the mean) from 6 rats/group at the end of feeding period. All real-time quantitative PCR reactions were carried out in duplicate. $^{b}P < 0.05$ versus the control group. (*E*) Western immunoblot analysis of expression of apoB in liver homogenates (containing 50 μg of total protein each). Control, rats pair-fed isocaloric liquid diet without ethanol; EtOH, ethanol-fed rats; PIO+EtOH, ethanol-fed rats given pioglitazone.

applied DNA microarrays to reveal differential mRNA expression between the livers exposed to chronic ethanol feeding with and without pioglitazone treatment. The transcriptome analysis allowed us to reveal up-regulation of c-Met (Figure 2*A*) and down-regulation of SCD-1 and -2, lipogenic enzymes in the liver (data not shown). Pioglitazone had no effect on the hepatic levels of TNF-α, UCP-2, CYP4A2 (cytochrome P450 4A2), CYP2E1, PPARγ, AMPK-catalytic subunit (α1 and α2), microsomal triglyceride transfer protein (MTTP), hepatic enzymes contributing to fatty acid oxidation such as carnitine palmitoyltransferase-1 or acyl-CoA oxidase (data not shown). These results were confirmed by real-time PCR analysis (Table 3). Chronic ethanol feeding significantly increased CYP2E1 mRNA and decreased PPARγ mRNA (Table 3).

Pioglitazone Increased Hepatic c-Met Expression and Induced Tyrosine Phosphorylation of c-Met Leading to Increased Hepatic apoB Expression

Alterations in c-Met gene expression were also confirmed at the protein levels. Moderate expression of c-Met protein was observed in the liver of the control rats, and the ethanol diet decreased the expression of c-Met protein (Figure 2*C*). The decrease in c-Met protein

Table 3. The Level of Expression of Genes Known to Play a Role in the Formation of Steatosis and Steatohepatitis Among the Treated Groups

Gene	Ethanol	Ethanol + Pioglitazone
TNF-α	1.12 ± 0.22	1.17 ± 0.23
UCP2	1.21 ± 0.30	1.18 ± 0.21
CYP2E1	[a]1.81 ± 0.32	[a]1.76 ± 0.24
CYP4A2	1.07 ± 0.36	1.11 ± 0.23
PPAR-α	[a]0.46 ± 0.12	[a]0.50 ± 0.09
AMPKα1	0.89 ± 0.31	0.95 ± 0.19
AMPKα2	1.14 ± 0.15	1.08 ± 0.17
Acyl-CoA oxidase	0.90 ± 0.28	0.95 ± 0.21
CPT-1	1.06 ± 0.17	1.10 ± 0.23
MTTP	0.94 ± 0.27	0.95 ± 0.26

NOTE. Results (and SEM) from 8 rats/group at the end of feeding period. Quantifications were normalized for RNA from the liver in the control group.
[a]$P < 0.05$ versus the control group.

in the liver of the ethanol-fed rats was restored by pioglitazone administration (Figure 2*C*). The level of tyrosine phosphorylation of c-Met was also reduced in the ethanol-fed liver, whereas the pioglitazone treatment attenuated this change (Figure 2*C*). DNA array and real-time PCR analyses also showed that ethanol administration decreased hepatic c-Met expression and that pioglitazone prevented this decrease (Figure 2*A*, *B*). Chronic ethanol feeding significantly increased HGF at both mRNA and protein levels, whereas the pioglitazone treatment did not alter these levels (Figure 2*D*). Western blotting analysis showed that the level of apoB 100 protein in the liver was increased by pioglitazone in the ethanol-fed rats (Figure 2*E*).

Stimulatory Effects of Pioglitazone on c-Met Expression, Its Tyrosine Phosphorylation, DNA Synthesis, and apoB Expression in Primary-Cultured Hepatocytes

To examine the direct effect of pioglitazone on expression of c-Met, rat primary cultured hepatocytes were incubated with various doses of pioglitazone and troglitazone for 24 hours (from 24 hours to 48 hours after inoculation). Ten μM pioglitazone markedly increased c-Met expression. The same concentration of troglitazone also increased c-Met expression, and the addition of bisphenol A diglycidyl ether (BADGE), a PPARγ antagonist,[22] inhibited this reaction (Figure 3*A*). The level of tyrosine phosphorylation was also increased by the addition of pioglitazone (Figure 3*B*). Stimulation of hepatocytes with both 5 ng/mL HGF and pioglitazone led to a greater increase in DNA synthesis than with either alone. In primary-cultured hepatocytes, HGF at 5 ng/mL and pioglitazone at 10 μmol/L maximally stimulated BrdU incorporation into DNA (Figure 3*C*). Pioglitazone also mimicked stimulatory effects of HGF on the expression of apoB in primary-cultured hepatocytes as seen in Figure 3*D* and *E*.

Troglitazone Mimicked the Actions of Pioglitazone In Vivo

In the in vivo study for troglitazone, we found that troglitazone significantly reduced fat accumulation and improved serum transaminase level in ethanol-fed rats. Troglitazone also enhanced hepatic c-Met expression (Figure 4).

Pioglitazone Decreased Hepatic SCD-1, 2, and SREBP-1c Expressions, Mimicking Effects of HGF

The real-time PCR analysis showed that chronic ethanol feeding conspicuously increased hepatic SCD-1 and 2 expressions, and that pioglitazone treatment suppressed them, consistent with the results of DNA array (Figure 5). Pioglitazone significantly decreased hepatic SREBP-1c expressions, although it had no effect on hepatic SREBP-1a level (Figure 5). Such effects of pioglitazone were also reproducible in primary-cultured hepatocytes. The HGF treatment dramatically decreased SREBP-1c and SCD-2 expressions in primary-cultured hepatocytes (Figure 6*A*). Pioglitazone treatment also decreased SREBP-1c and SCD-2 expressions upon the application of HGF, although the reagent had no effect on them without it (Figure 6*B*, *C*).

Pioglitazone Attenuates Hepatic Lipid Peroxidation Elicited by Chronic Ethanol Feeding

4-HNE-adducted protein, as a product of lipid peroxidation reaction, was intensely detected in centrilobular regions of ethanol-fed rats and colocalized with accumulated lipid droplets. The pioglitazone treatment decreased the products of lipid peroxidation (Figure 7*A*). We found by real-time PCR analysis that the hepatic level of stress response proteins such as metallothionein (MT) -1, -2, and heme oxygenase (HOX)-1 dramatically increased in ethanol-fed rats (group A). Pioglitazone prevented these stress responses induced by ethanol (Figure 7*B*). Of importance in the current study is that neither the pioglitazone treatment nor chronic ethanol feeding induced any notable apoptosis, as judged by the TUNEL method seen in Figure 7*C*.

In this study, all rats in the groups were pair fed daily on an isoenergetic basis, and the rats in group A and B were daily given the same amounts of ethanol. We then inquired

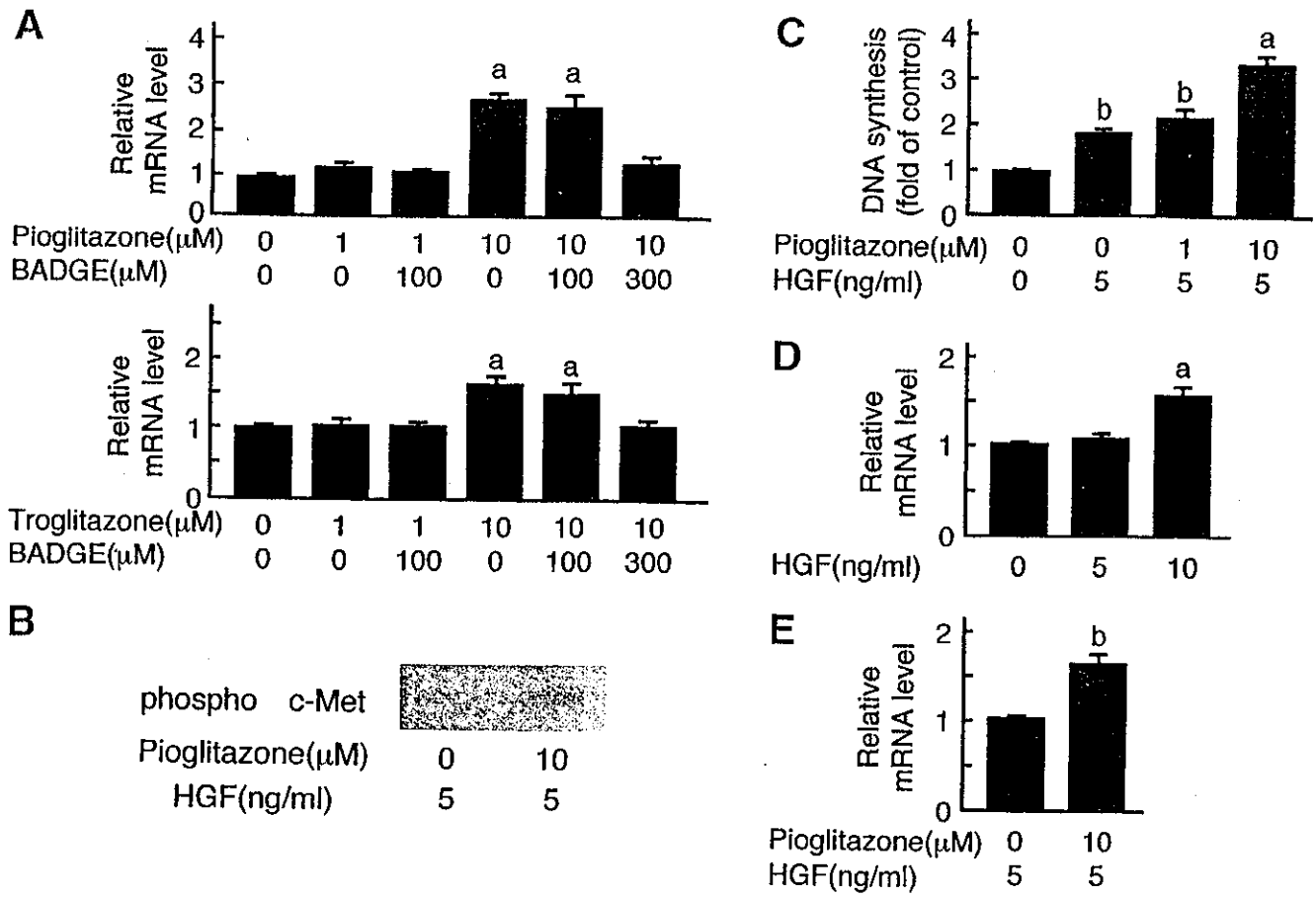

Figure 3. Direct effect of pioglitazone on expression and tyrosine phosphorylation of c-Met, expression of apoB, and on DNA synthesis in rat primary cultured hepatocytes. (*A*) Rat primary-cultured hepatocytes were incubated with various doses of pioglitazone or troglitazone for 24 hours (from 24 to 48 hours after inoculation). In the control, the medium was supplemented with the same volume of DMSO. Real-time quantitative PCR analysis of c-Met showed that 10 μmol/L of pioglitazone treatment dramatically increased c-Met expression. Ten μmol/L of troglitazone treatment also significantly increased c-Met expression. Addition of 300 μmol/L of BADGE inhibited this increase. All real-time quantitative PCR reactions were carried out in duplicate. Results (and standard error of the mean) from 4 individual experiments. $^{a}P < 0.05$ versus the groups with 0 or 1 μmol/L of pioglitazone or troglitazone treatment. (*B*) Tyrosine phosphorylation of c-Met in homogenates of primary-cultured hepatocytes stimulated or not with 5 ng/mL HGF or pioglitazone. Addition of 10 μmol/L pioglitazone induced tyrosine phosphorylation of c-Met. (*C*) Effect of pioglitazone on DNA synthesis of primary cultured hepatocytes. BrdU incorporation into cellular DNA was determined 24 hours after the addition of HGF and/or pioglitazone. $^{a}P < 0.05$ versus the other groups. $^{b}P < 0.05$ versus the groups without any addition of HGF or pioglitazone. Next, real-time PCR analysis of primary-cultured hepatocytes was used to assess apoB gene expression (*D*, *E*). (*D*) Rat primary-cultured hepatocytes were incubated with various doses of HGF for 24 hours. $^{a}P < 0.05$ versus the group without addition of HGF. (*E*) Incubation with pioglitazone with addition of 5 ng/mL of HGF for 24 hours. $^{b}P < 0.05$ versus the group without any addition of pioglitazone. All real-time quantitative PCR reactions were carried out in duplicate. Results (and standard error of the mean) from 4 individual experiments.

whether the treatment with pioglitazone by itself could alter ethanol metabolism in rats. Table 4 shows that blood levels of ethanol and acetaldehyde did not differ significantly irrespective of the presence or absence of pioglitazone in ethanol-fed rats. This result suggests that pioglitazone has little, if any, effect on ethanol metabolism and thus is not a likely mechanism for the attenuating effect of this reagent on hepatic steatosis.

Discussion

This study first suggested that pioglitazone serves as a potentially therapeutic tool to attenuate hepatic steatosis caused by chronic administration of ethanol. Furthermore, several lines of evidence provided in this study suggest that the ability of this antidiabetic to significantly alter synthesis and redistribution of lipids is ascribable to therapeutic potential against the ethanol-induced hepatic steatosis. The epididymal fat weight/body weight ratio significantly decreased in the ethanol-fed rats compared with that in the pair fed rats. Distinct from nonalcoholic hepatic steatosis, which induced by chronic alcohol abuse often coincided with energy wasting and inhibition of adipose tissue accumulation. These events are likely to result in the fact that alcoholics are

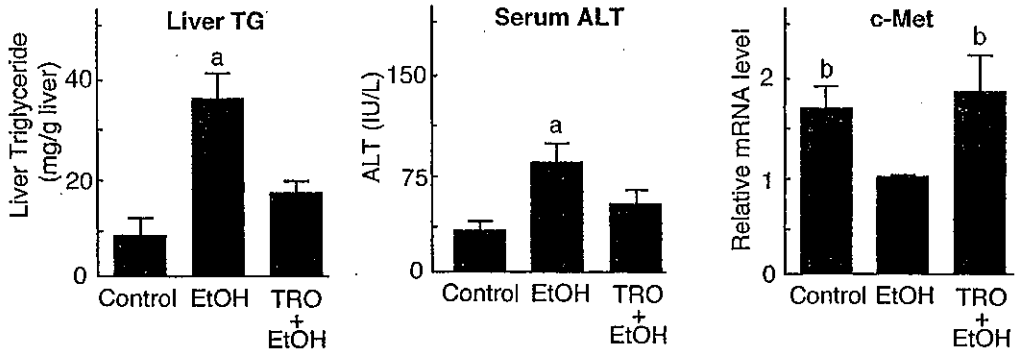

Figure 4. Troglitazone mimicked the actions of pioglitazone in vivo. Eight-week-old male SD rats fed ethanol-containing liquid diet were given troglitazone (200 mg/kg body weight per day) once every 24 hours intragastrically for 6 weeks. In this study, we divided the rats into 3 groups in the same way as our last examination of pioglitazone (n = 6). Troglitazone decreased accumulation of lipid droplets and suppressed the elevation of serum concentrations of ALT in ethanol-fed rats. Real-time PCR analyses showed that ethanol administration decreased hepatic c-Met expression and that troglitazone prevented this decrease. Results (and standard error of the mean) from 6 rats/group at the end of feeding period. All real-time quantitative PCR reactions were carried out in duplicate. $^{a}P < 0.05$ versus the other groups. $^{b}P < 0.05$ versus the ethanol-fed group. Control, rats pair-fed isocaloric liquid diet without ethanol; EtOH, ethanol-fed rats; TRO+EtOH, ethanol-fed rats given troglitazone.

not obese despite a high total energy intake.[23] Pioglitazone prevented the decrease in amount of adipose tissue, probably by mobilizing fat from the liver to adipose tissue.

It has been believed until now that impaired mitochondrial β-oxidation of fatty acids could be a major cause of triglyceride accumulation in alcoholic fatty liver.[24] In the current study, however, pioglitazone did not alter the expression of hepatic enzymes contributing to fatty acid oxidation such as carnitine palmitoyltransferase-1 or acyl-CoA oxidase (AOX) or the expression of hepatic TNF-α, uncoupling protein-2, PPARγ, or AMPK-catalytic subunit (α1 and α2) levels; plasma TNF-α, glucose, leptin, insulin levels, or insulin resistance remained unchanged. These results suggest that other mechanisms play central roles in pioglitazone's effect on alcoholic fatty liver. Differential

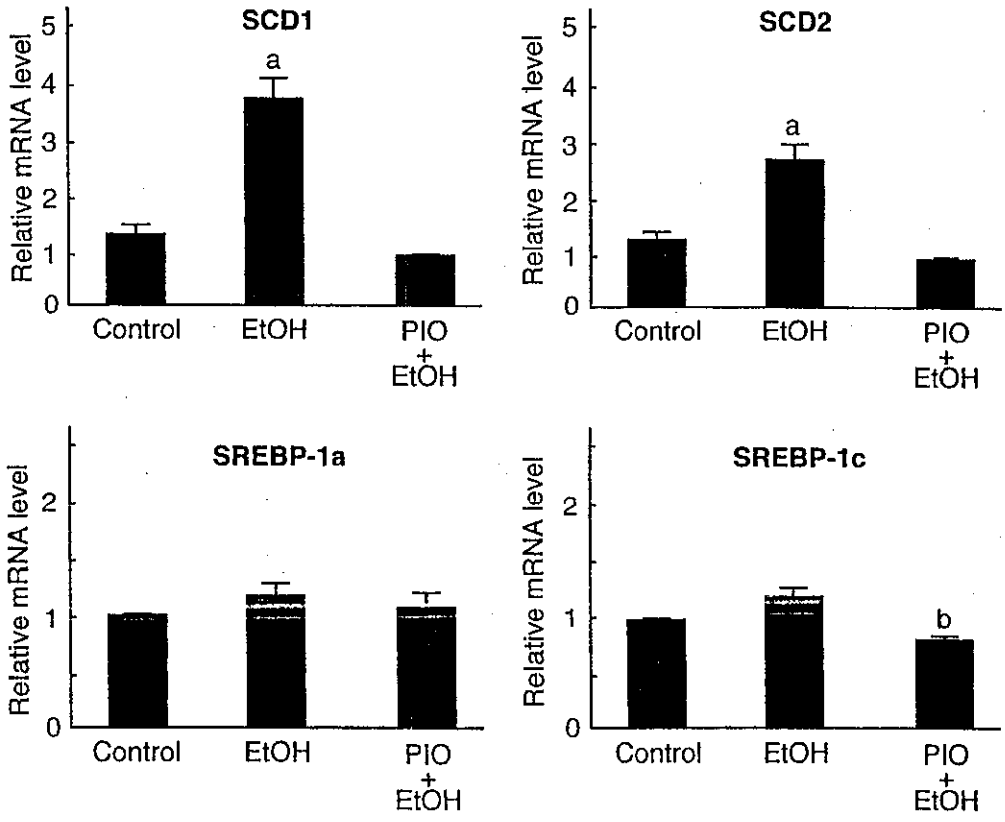

Figure 5. Hepatic SCD1, SCD2, SREBP-1a, and SREBP-1c expression. Real-time PCR analysis was carried out to quantitate hepatic mRNA levels of SCD1, SCD2, SREBP-1a, and SREBP-1c in liver homogenates among the groups. Results (and standard error of the mean) from 4 rats/group at the end of feeding period. All real-time quantitative PCR reactions were carried out in duplicate. $^{a}P < 0.05$ versus the other groups. $^{b}P < 0.05$ versus the ethanol-fed group. Control, rats pair-fed isocaloric liquid diet without ethanol; EtOH, ethanol-fed rats; PIO+EtOH, ethanol-fed rats given pioglitazone.

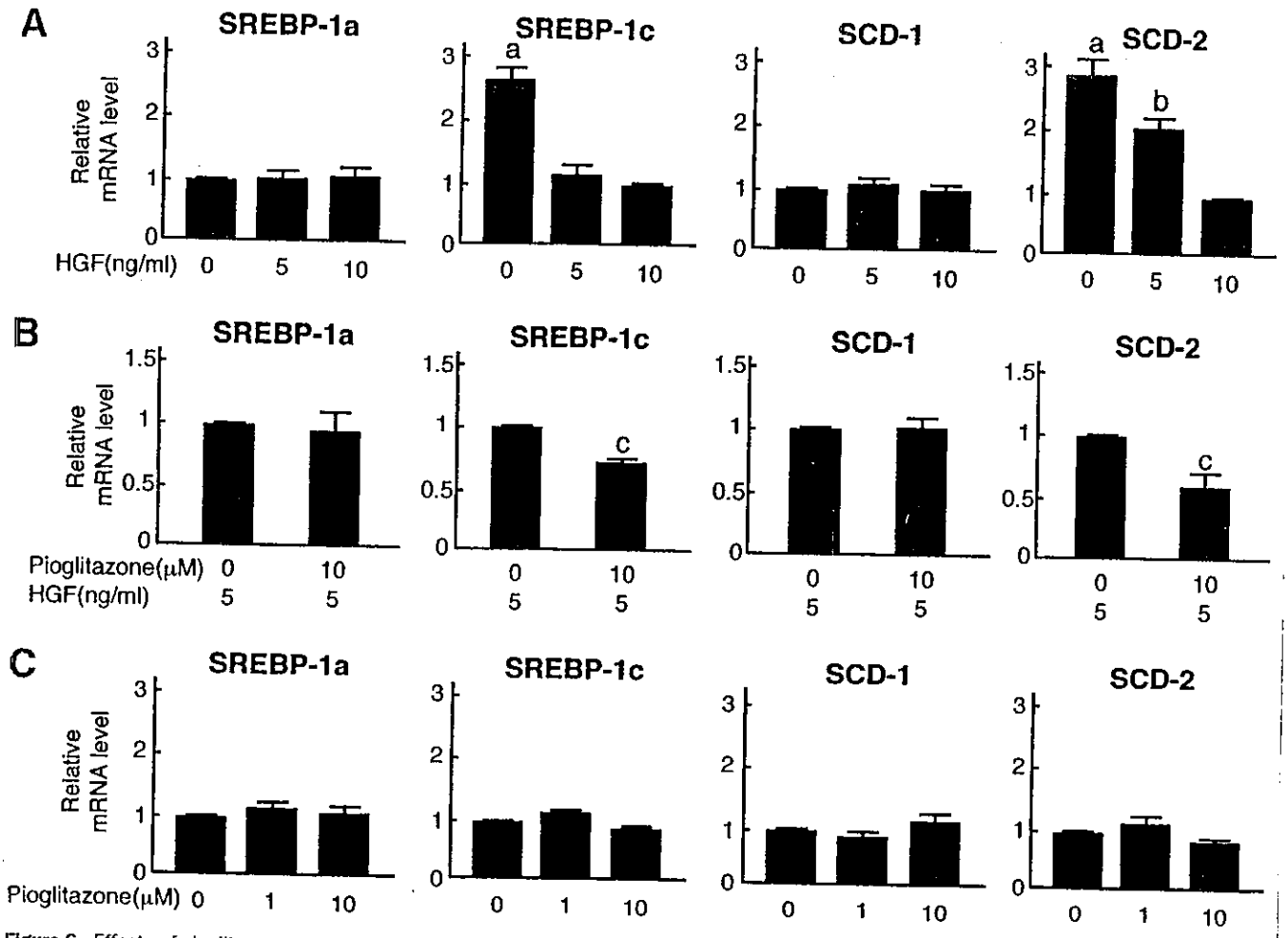

Figure 6. Effects of pioglitazone and HGF on expression of SREBP-1a, c, and SCD-1, 2 mRNA in hepatocyte cultures. Real-time PCR analysis was used to assess SREBP-1a, SREBP-1c, SCD-1, and SCD-2 gene expression. (*A*) Rat primary-cultured hepatocytes were incubated with various doses of HGF for 24 hours. $^{a}P < 0.05$ versus the other groups. $^{b}P < 0.05$ versus the group with addition of 10 ng/mL of HGF. (*B*) Incubation with pioglitazone with addition of 5 ng/mL of HGF for 24 hours. $^{c}P < 0.05$ versus the group without any addition of pioglitazone. (*C*) Incubation with various doses of pioglitazone for 24 hours. All real-time quantitative PCR reactions were carried out in duplicate. Results (and standard error of the mean) from 4 individual experiments.

transcriptome analyses comparing mRNA expression in the chronic ethanol-exposed livers with and without the pioglitazone treatment led us to pinpoint a critical role of the hepatic c-Met signaling pathway, and the results suggest that the reagent facilitates HGF-induced intracellular signaling without altering hepatic HGF levels.

HGF is the most potent stimulator of hepatocyte proliferation.[25] HGF has multiple biological properties in the liver, including mitogenic, antifibrotic, antiapoptotic, and cytoprotective activities.[26–28] Such multiple biological responses elicited by HGF are transferred through the cytoplasmic domain of c-Met, a specific cell surface transmembrane tyrosine kinase receptor.[26] Observation that pioglitazone directly enhanced both c-Met and its activated form in rat primary cultured hepatocytes from ethanol-fed rats suggests that this reagent serves as the first clinically available tool that directly up-regulates c-Met expression in hepatocytes. Several data in the current study suggested that PPARγ is involved in mechanisms by which the reagent up-regulates c-Met, inasmuch as this event is mimicked by troglitazone, another PPARγ ligand, and is canceled by BADGE, a PPARγa antagonist. Further studies are necessary to determine the whole mechanisms for exploring direct actions of the reagent on c-Met expression.

HGF is known to stimulate apoB secretion in hepatocytes and to induce cell maturation during liver regeneration.[29] The HGF administration has recently been shown to improve alcoholic fatty liver by enhancing apoB synthesis and subsequent mobilization of lipids from hepatocytes with fatty changes.[13] These observations led us to examine if pioglitazone could serve as a

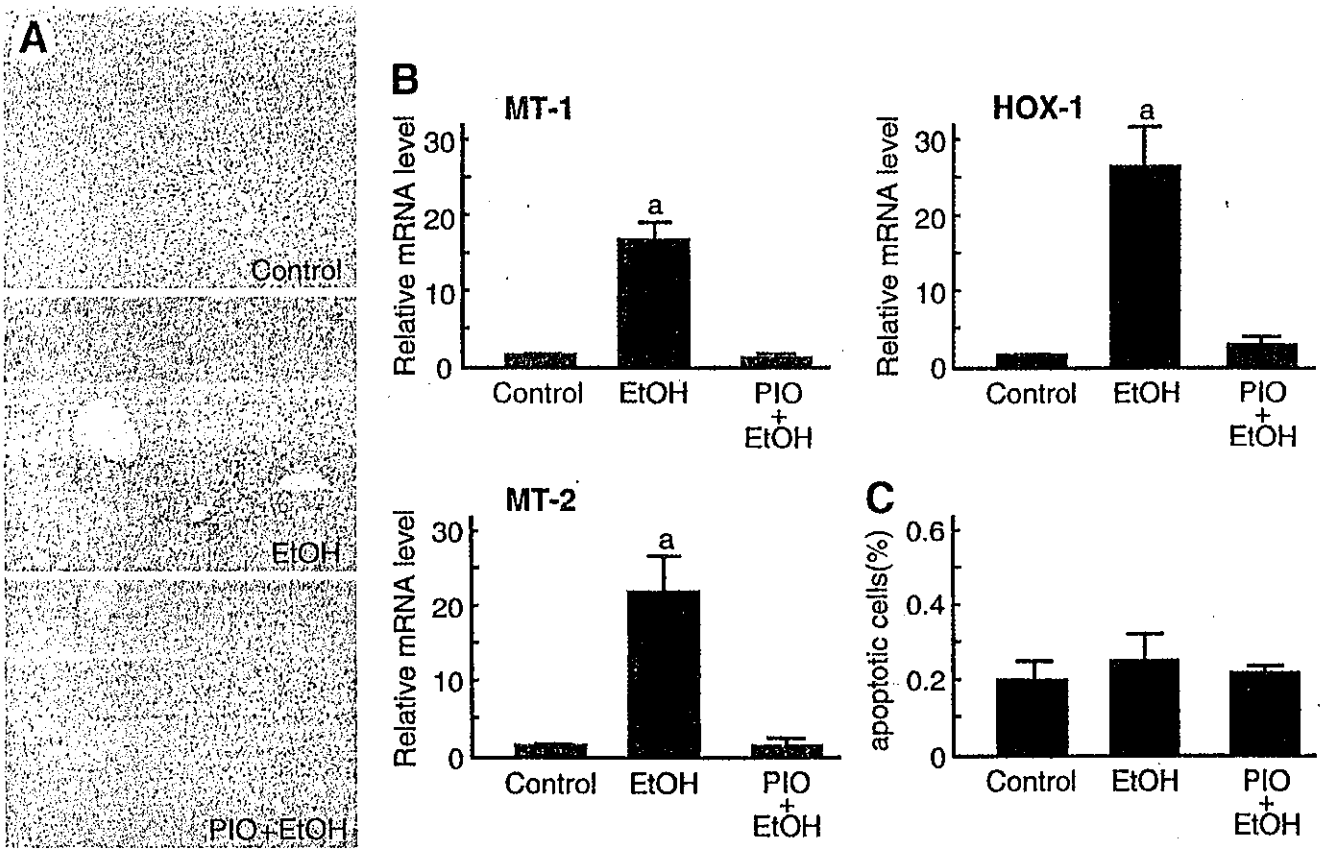

Figure 7. Effect of pioglitazone on hepatic lipid peroxidation, apoptosis, and expression of stress response proteins. (*A*) Immunohistochemistry for 4-HNE. Representative liver samples of control rat (Cont), ethanol-fed rats (EtOH), and ethanol-fed rats given pioglitazone (EtOH+Piog) (×100). (*B*) Real-time PCR analysis was used to assess stress response proteins such as MT-1, MT-2, and HOX-1 mRNA expression in liver homogenates among the groups. Results (and standard error of the mean) from 4 rats/group at the end of feeding period. All real-time quantitative PCR reactions were carried out in duplicate. $^{a}P < 0.05$ versus the other groups. (*C*) TUNEL results of liver apoptosis among the treated groups. The apoptotic cells and hepatocytes were counted from 5 lower microscopic fields for each animal.

substitute reagent that triggers lipid mobilization from the liver through stimulation of the c-Met pathway. As one might expect, the current results showed that pioglitazone mimics such effects of HGF to stimulate hepatic apoB synthesis and resultant VLDL secretion through HGF/c-Met intracellular signaling; this event could greatly contribute to mobilization of triglycerides from the liver undergoing chronic ethanol exposure.

Table 4. Blood Concentration of Ethanol and Acetaldehyde in Pioglitazone-Treated and Control Rats After Ethanol Administration (4 g/kg)

		Control	Pioglitazone Treated
Ethanol (mg/dL)	0 h	0 ± 0	0 ± 0
	2 h	184 ± 27	198 ± 26
	12 h	82 ± 22	84 ± 35
	24 h	3 ± 1	4 ± 2
Acetaldehyde (mg/L)	0 h	0 ± 0	0 ± 0
	2 h	1.9 ± 0.5	2.0 ± 0.4
	12 h	0.2 ± 0.1	0.2 ± 0.1
	24 h	0 ± 0	0 ± 0

Besides its action on lipid mobilization from the liver, pioglitazone obviously exerts its anti-steatotic actions through multiple mechanisms as judged by alterations in expression of genes responsible for triglyceride synthesis. SREBPs and stearoyl-CoA (SCD) are such genes responding to pioglitazone. Ntambi et al.[30] recently reported that a lipogenic diet fed to mice with a null mutation in the SCD1 gene (SCD1-/-) failed to induce the synthesis of triglycerides in liver, despite the induction of expression of SREBP-1 and its target genes. Cohen et al.[31] also reported that SCD-1 is required for the fully developed obese phenotype of leptin-deficient mice, including fatty liver. SCD-1 and SCD-2 catalyze the same reaction, and SCD-2 is reported to be expressed at higher levels in livers of mice overexpressing the truncated nuclear form of SREBP-1.[32] These observations suggest that induction of triglyceride synthesis is highly dependent on SCD

gene expression and that both SCD-1 and SCD-2 play a role in the mechanism of fatty liver. As shown in results from our and other laboratories, chronic ethanol feeding increased levels of SCD-2, and SREBP-1c expression. Consistent with our results, Crabb et al.[33] recently reported that chronic ethanol feeding activates hepatic SREBP-1. Such suppressive actions of pioglitazone on up-regulation of these genes could greatly improve ethanol-induced hepatic steatosis cooperatively with its aforementioned effects on the lipid mobilization via VLDL as a whole.

Recently, HGF was reported to prevent LPS-induced hepatic sinusoidal endothelial cell injury and intrasinusoidal fibrin deposition in rats.[34] It has also been reported that the mere presence of fat in the liver leads to hepatic lipid peroxidation and that chronic steatosis is associated with persistent lipid peroxidation.[35] Lipid peroxidation is proposed as a mechanism of alcohol-induced hepatotoxicity. It has been suggested that chronic lipid peroxidation could represent the missing link between chronic steatosis and steatohepatitis. In our study, pioglitazone improved ethanol-induced lipid peroxidation and resultant cellular damages by increasing the c-Met expression and by decreasing hepatic fat amounts, as indicated by results showing suppression of antioxidative genes such as MT-1, -2, and HOX-1.[36,37] Furthermore, so far as judged from the current TUNEL analyses, pioglitazone treatment did not induce any notable apoptosis in liver. Such a cytoprotective feature of pioglitazone on ethanol-induced hepatic steatosis is likely to be of great clinical advantage in that other thiazolidinedione derivatives such as troglitazone have been reported to induce apoptotic hepatocyte death, leading to a conflict for its clinical use.[38] Based on these findings, we propose an important new mechanism to explain the recovery from alcoholic fatty liver in response to pioglitazone (i.e., that pioglitazone enhances c-Met expression in hepatocytes, resulting in activation of HGF/c-Met signaling). The HGF/c-Met signaling activation induced by pioglitazone leads to increased apoB synthesis with subsequent lipid mobilization of VLDL from hepatocytes, and decreases hepatic SCD levels with decreased synthesis of triglycerides in liver. Such an effect of pioglitazone could also stimulate regeneration and attenuate lipid peroxidation.

The current study suggesting usefulness of pioglitazone to treat ethanol-induced hepatic steatosis led us to hypothesize that such an HGF-mimicking hepatoprotective PPARγ ligand could clinically be used to limit fatty infiltration of the liver caused by other disease conditions. For instance, posttransplant fatty infiltration in the donor liver accounts for a serious complication causing primary nonfunction.[39] Because use of steatotic livers are actually increasing for transplantation because of a shortage of the nonsteatotic donor grafts, we should find the method for amelioration of injury in donor fatty liver at liver transplantation. A possible use of the pioglitazone treatment deserves future studies if its use for posttransplanted recipients or for nonalcoholic steatohepatitis turned out to reduce the related liver injury. This may provide a means for designing future therapeutic strategies with pioglitazone. Pioglitazone may thus be useful as a therapeutic agent for alcoholic fatty liver and merits further evaluation.

References

1. Sorensen TI, Orholm M, Bentsen KD, Hoybye G, Eghoje K, Christoffersen P. Prospective evaluation of alcohol abuse and alcoholic liver injury in men as predictors of development of cirrhosis. Lancet 1984;2:241–4.
2. Teli MR, Day CP, Burt AD, Bennett MK, James OFW. Determinants of progression to cirrhosis or fibrosis in pure alcoholic fatty liver. Lancet 1995;346:987–990.
3. Lin HA, Yang SQ, Chuckaree C, Kuhajda F, Ronnet G, Diehl AM. Metformin reverses fatty liver disease in obese, leptin-deficient mice. Nat Med 2000;6:998–1003.
4. Zhou G, Myers R, Li Y, Chen Y, Shen X, Fenyk-Melody J, Wu M, Ventre J, Doebber T, Fujii N, Musi N, Hirshman MF, Goodyear LJ, Moller DE. Role of AMP-activated protein kinase in mechanism of metformin action. J Clin Invest 2001;108:1167–1174.
5. Shimabukuro M, Zhou YT, Lee Y, Unger RH. Troglitazone lowers islet fat and restores beta cell function of Zucker Diabetic Fatty rats. J Biol Chem 1998;273:3547–3550.
6. Higa M, Zhou YT, Ravazzola M, Baetens D, Orci L, Unger RH. Troglitazone prevents mitochondrial alterations, β cell destruction, and diabetes in obese prediabetic rats. Proc Natl Acad Sci U S A 1999;96:11513–11518.
7. Kakuma T, Lee Y, Higa M, Wang ZW, Pan W, Shimomura I, Unger RH. Leptin, troglitazone, and the expression of sterol regulatory element binding proteins in liver and pancreatic islets. Proc Natl Acad Sci U S A 2000;97:8536–8541.
8. Scheen AJ. Hepatotoxicity with thiazolidinediones: is it a class effect? Drug Saf 2001;24:873–888.
9. Lieber CS, DeCarli LM, Sorrell MF. Experimental methods of ethanol administration. Hepatology 1989;10:501–510.
10. Maeshida Y, Kiyota Y, Yoshimura Y, Motohashi M, Tanayama S. Disposition of the new antidiabetic agent pioglitazone in rats, dogs, and monkeys. Arzneim.-Forsch/Drug Res 1997;47:29–35.
11. Hayakawa T, Shiraki T, Morimoto T, Shii K, Ikeda H. Pioglitazone improves insulin signaling defects in skeletal muscle from Wistar fatty (fa/fa) rats. Biochem Biophys Res Commun 1996;223:439–444.
12. Horikoshi H, Yoshioka T, Kawasaki T, Nakamura K, Matsunuma N, Yamaguchi K, Sasahara K. Troglitazone (CS-045), a new antidiabetic drug. Annu Rep Sankyo Res Lab 1994;46:1–57.
13. Tahara M, Matsumoto K, Nukiwa T, Nakamura T. Hepatocyte growth factor leads to recovery from alcohol-induced fatty liver in rats. J Clin Invest 1999;103:313–320.
14. Bachorik PS, Ross JW. National cholesterol education program recommendations for measurement of low-density lipoprotein cholesterol: executive summary. Clin Chem 1995;41:1414–1420.

15. Hatch FT, Lees RS. Practical methods for plasma lipoprotein analysis. Adv Lipid Res 1968;6:1–68.
16. Tomita K, Sato M, Kajiwara K, Tanaka M, Tamiya G, Makino S, Tomizawa M, Mizutani A, Kuwano Y, Shiina T, Ishii H, Kimura M. Gene structure and promoter for *Crad2* encoding mouse cis-retinol/3α-hydroxysterol short-chain dehydrogenase isozyme. Gene 2000;251:175–186.
17. Dunn JCY, Yarmush ML, Koebe HG, Tompkins RG. Hepatocyte function and extracellular matrix geometry: long-term culture in a sandwich configuration. FASEB J 1989;3:174–177.
18. Lawrence JM, Reckless JP. Actos (pioglitazone): a new treatment for type 2 diabetes. Hosp Med 2001;62:411–416.
19. Pellizzari CA, Khodarev NN, Gupta N, Calvin DP, Weichselbaum RR. Quantitative analysis of DNA array autoradiographs. Nucleic Acids Res 2000;28:4577–4581.
20. Tenenbaum SA, Carson CC, Lager PJ, Keene JD. Identifying mRNA subsets in messenger ribonucleoprotein complexes by using cDNA arrays. Proc Natl Acad Sci U S A 2000;97:14085–14090.
21. Okada T, Mizoi Y. Studies on the problem of blood acetaldehyde determination in man and level after alcohol intake. Jpn J Alcohol Drug Depend 1982;17:141–159.
22. Wright HM, Clish CB, Mikami T, Hauser S, Yanagi K, Hiramatsu R, Serhan CN, Spiegelman BM. A synthetic antagonist for the peroxisome proliferator-activated receptor gamma inhibits adipocyte differentiation. J Biol Chem 2000;275:1873–1877.
23. Levine JA, Harris MM, Morgan MY. Energy expenditure in chronic abuse. Eur J Clin Invest 2000;30:779–786.
24. Eaton S, Record CO, Bartlett K. Multiple biochemical effects in the pathogenesis of alcoholic fatty liver. Eur J Clin Invest 1997;27:719–722.
25. Michalopoulos GK, Defrances MC. Liver regeneration. Science 1997;276:60–66.
26. Stuart KA, Riordan SM, Lidder S, Crostella L, Williams R, Skouteris GG. Hepatocyte growth factor/scatter factor-induced intracellular signaling. Int J Exp Pathol 2000;81:17–30.
27. Takehara T, Nakamura T. Protective effect of hepatocyte growth factor on *in vitro* hepatitis in primary cultured hepatocytes. Biomed Res 1991;12:335–338.
28. Ishiki Y, Ohnishi H, Muto Y, Matsumoto K, Nakamura T. Direct evidence that hepatocyte growth factor is a hepatotropic factor for liver regeneration and has a potent antihepatitis effect in vivo. Hepatology 1992;16:1227–1235.
29. Kaibori M, Kwon AH, Oda M, Kamiyama Y, Kitamura N, Okumura T. Hepatocyte growth factor stimulates synthesis of lipids and secretion of lipoproteins in rat hepatocytes. Hepatology 1998;27:1354–1361.
30. Ntambi JM, Miyazaki M, Stoehr JP, Lan H, Kendziorski CM, Yandell BS, Song Y, Cohen P, Friedman JM, Attie AD. Loss of stearoyl-CoA desaturase-1 function protects mice against adiposity. Proc Natl Acad Sci U S A 2002;99:11482–11486.
31. Cohen P, Miyazaki M, Socci ND, Hagge-Greenberg A, Liedtke W, Soukas AA, Sharma R, Hudgins LC, Ntambi JM, Friedman JM. Role for stearoyl-CoA desaturase-1 in leptin-mediated weight loss. Science 2002;297:240–243.
32. Shimomura I, Shimano H, Korn BS, Bashmakov Y, Horton JD. Nuclear sterol regulatory element-binding proteins activate genes responsible for the entire program of unsaturated fatty acid biosynthesis in transgenic mouse liver. J Biol Chem 1998;273:35299–35306.
33. You M, Fischer M, Deeg MA, Crabb DW. Ethanol induces fatty acid synthesis pathways by activation of sterol regulatory element-binding protein (SREBP). J Biol Chem 2002;277:29342–29347.
34. Sato S, Kaido T, Yamaoka S, Yoshikawa A, Arii S, Nakamura T, Niwano M, Imamura M. Hepatocyte growth factor prevents lipopolysaccharide-induced hepatic sinusoidal endothelial cell injury and intrasinusoidal fibrin deposition in rats. J Surg Res 1998;80:194–199.
35. Letteron P, Fromenty B, Terris B, Degott C, Pessayre D. Acute and chronic hepatic steatosis lead to in vivo lipid peroxidation in mice. J Hepatol 1996;24:200–208.
36. Kyokane T, Norimizu S, Taniai H, Yamaguchi T, Takeoka S, Tsuchida E, Naito M, Nimura Y, Ishimura Y, Suematsu M. Carbon monoxide from heme catabolism protects against hepatobiliary dysfunction in endotoxin-treated rat liver. Gastroenterology 2001;120:1227–1240.
37. Hayashi S, Takamiya R, Yamaguchi T, Matsumoto K, Tojo SJ, Tamatani T, Kitajima M, Makino N, Ishimura Y, Suematsu M. Induction of heme oxygenase-1 suppresses venular leukocyte adhesion elicited by oxidative stress: role of bilirubin generated by the enzyme. Circ Res 1999;85:663–671.
38. Yamamoto Y, Nakajima M, Yamazaki H, Yokoi T. Cytotoxicity and apoptosis produced by troglitazone in human hepatoma cells. Life Sci 2001;70:471–482.
39. Imber CJ, Peter SDS, Handa A, Friend PJ. Hepatic steatosis and its relationship to transplantation. Liver Transpl 2002;8:415–423.

Received March 8, 2003. Accepted December 4, 2003.

Address reprint requests to: Hiromasa Ishii, M.D., Department of Internal Medicine, School of Medicine, Keio University, 35 Shinanomachi, Shinjuku-ku, Tokyo 160-8582, Japan. e-mail: hishii@sc.itc.keio.ac.jp; fax: (81) 3-3356-9654.

Supported by a grant from Keio University, School of Medicine, Nateglinide Memorial Toyoshima Research and Education Fund, and the 21st Century Center-Of-Excellence (COE) Program from Ministry of Education, Culture, Sports, Science, and Technology.

The authors thank T. Saito, H. Ochiai, M. Tomizawa, and E. Tokubo for technical assistance.

Available online at www.sciencedirect.com
SCIENCE DIRECT®
Hepatology Research 28 (2004) 102–108
Hepatology Research
www.elsevier.com/locate/ihepcom

Ethanol upregulates pro-fibrogenic connective tissue growth factor (CTGF) gene expression in HepG2 cells via cytochrome P450 2E1-mediated ethanol oxidation

Masahiro Konishi [a,*], Shinzo Kato [a], Mikio Kajihara [a], Arthur Cederbaum [b], Hiromasa Ishii [a]

[a] *Department of Internal Medicine, Keio University School of Medicine, 35 Shinanomachi, Shinjuku-ku, Tokyo 160-8582, Japan*
[b] *Department of Biochemistry and Molecular Biology, Mount Sinai School of Medicine, New York, NY, USA*

Received 13 November 2003; received in revised form 11 December 2003; accepted 15 December 2003

Abstract

Connective tissue growth factor (CTGF) is a pro-fibrogenic molecule involved in several human fibrotic disorders. CTGF overexpression in the liver, through upregulation of CTGF mRNA in hepatic stellate cells (HSCs), is reported to correlate with the degree of fibrosis. Although alcohol is a major cause of hepatic fibrosis, the role of CTGF in alcoholic hepatic fibrogenesis, has been poorly understood. Oxidative stress, mediated by ethanol-inducible Cytochrome P-4502E1(CYP2E1), has been implicated as a crucial factor in alcoholic hepatic fibrogenesis. Therefore, we investigated the contribution of CYP2E1-mediated ethanol oxidation to CTGF mRNA expression by using a well-established HepG2 cell line constitutively expressing CYP2E1 (E9 cells). CTGF mRNA quantitation by a real-time reverse polymerase chain reaction (RT-PCR) showed a significant increase in CTGF mRNA levels in ethanol-treated E9 cells. Phorbol myristate acetate (PMA), which enhances CYP2E1 expression, increased CTGF mRNA levels. This increase was diminished after co-incubation with 4-methylpyrazole (4MP), a CYP2E1 inhibitor, or an antioxidant, *N*-acetylcysteine. We visualized the state of oxidative stress only in ethanol-treated E9 cells by a newly-established anti-acrolein-modified antibody. In conclusion, our study has first identified a possible role of CYP2E1-mediated ethanol oxidation in CTGF gene upregulation, suggesting a considerable role of CTGF in alcoholic hepatic fiberogenesis.

Keywords: Fibrosis; Oxidative Stress; Real-time RT-PCR; Acrolein

1. Introduction

Connective tissue growth factor (CTGF) is a multi-functional matricellular peptide that was originally identified from human vascular endothelial cells in culture [1]. It belongs to the CCN gene family, which includes CTGF, Cyr61/Cef10, Elm1, and Nov [2–5]. These genes are thought to exert, as immediate early growth-responsive genes, diverse cellular functions, such as cell proliferation, differentiation, apoptosis, adhesion, and embryogenesis [6,7].

CTGF mRNA and protein are over-expressed in numerous human fibrotic disorders of the lung [8], liver [6], kidney [9,10], pancreas [11], bowel [12], skin [7,13], and eyes [14]; thus its role to promote fibrosis has attracted much attention [6,7]. Hepatic fibrosis, the ultimate form of chronic liver diseases, is characterized by cell proliferation and excessive extracellular matrix (ECM) deposition [6]; in vitro, CTGF stimulates fibroblast proliferation and ECM synthesis. Recent studies, in vivo, using the liver biopsy specimens from patients with chronic viral (hepatitis B and hepatitis C) or alcoholic hepatic fibrosis revealed a significant correlation between CTGF immunostaining intensity and severity of fibrosis [6].

Transforming growth factor-β (TGF-β) not only induces collagen and ECM synthesis in the liver [7] but also regulates other biologically active pro-fibrotic mediators, such as CTGF. Indeed, the CTGF gene has a unique TGF-β-responsive element in its promoter [15]; it is conceivable that CTGF plays a role as a downstream mediator of some of the pro-fibrotic actions of TGF-β.

Hepatic stellate cells (HSCs) play a crucial role in hepatic fibrosis since these cells undergo activation with ECM deposition during fibrogenesis [15–22]. TGF-β initiates activation of HSCs in culture and induces CTGF expression.

* Corresponding author. Tel.: +81-3-3353-1211x62298; fax: +81-3-3353-6247.
E-mail address: k-show@ja2.so-net.ne.jp (M. Konishi).

1386-6346/$ – see front matter © 2004 Elsevier B.V. All rights reserved.
doi:10.1016/j.hepres.2003.12.003

CTGF mRNA expression is stimulated not only by TGF-β alone but also CTGF itself in HSC T6 cells [8]. In mouse fibroblasts, CTGF mRNA expression is stimulated by TGF-β, ethanol, or acetaldehyde. Co-incubating HSCs from fa/fa rats with glucose or insulin enhances CTGF expression, independent of TGF-β actions [23]. These data, taken together, suggest both autocrine or paracrine pathways of the CTGF action on HSCs are likely since exogenous CTGF is able to modulate HSC function. Thus, the underlying mechanisms which regulate CTGF expression in other cell types as well as HSCs in the liver await further investigations.

In alcoholic hepatic fibrogenesis, induction of oxidative stress response has been implicated as one of the major driving factors [24–31]. Microsomal ethanol oxidizing system containing Cytochrome P-4502E1 (CYP2E1), an effective producer of reactive oxygen species (ROS), is strikingly inducible by chronic and excessive ethanol consumption, which results not only in an increased production of acetaldehyde but also in the generation of substantial amount of superoxide as well as hydroxy and other free radicals. In HSCs, CYP2E1 is present at levels of only 4% or less those found in hapatocytes. Therefore, CYP2E1-mediated oxidative stress as a result of chronic and excessive ethanol consumption is more centered in hapatocytes rather than in HSCs [32,33].

Cederbaum, et al developed the HepG2 cell line stably expressing CYP2E1, namely E9. By using the cultured E9 cells, we explored the impact of CYP2E1-mediated ethanol oxidation on CTGF gene expression [34–37].

2. Materials and methods

2.1. Cell lines

Two human hepatoma HepG2 sublines were established and provided by Dr. Arthur Cederbaum; HepG2-MVh2E1-9 (E9) which has been transduced to stably overexpress 2E1 (Fig. 1) and HepG2-MV-5 (MV-5) which contains only a retroviral shuttle vector lacking the human CYP2E1 complementary DNA (cDNA). MV-5 cells do not express detectable CYP2E1. The *p*-nitrophenol oxidation activity of E9 cells was measured and E9 cells were used for the experiment only when the activity was maintained at the levels of 50–100 pmol/min/mg microsomal protein. Protein concentration was determined using the modified Lowry protein assay reagent kit (PERBIO, Rockford, IL).

Both cells were grown in minimum essential medium (MEM), 10% fetal bovine serum (FBS) and 0.1 mg/ml G418, supplemented with 1% penicillin-streptomycin-neomycin antibiotics, under standard culture conditions (5% CO_2, 37 °C). Cells were subcultured at a 1:5 ratio once a week.

2.2. Cell treatment with ethanol

During the actual treatment with ethanol, 1×10^6–2×10^6 cells were seeded on each well of a 6-well plate (Iwaki Glass, Tokyo, Japan) and incubated in 5% CO_2 at 37 °C. Hepatozyme, a commercial serum-free replacement (GIBCO BRL, Rockville, MD), which supports the growth of human hepatoma cells very well, was used as a culture medium. No hepatotoxicity was noted when the cells were cultured with

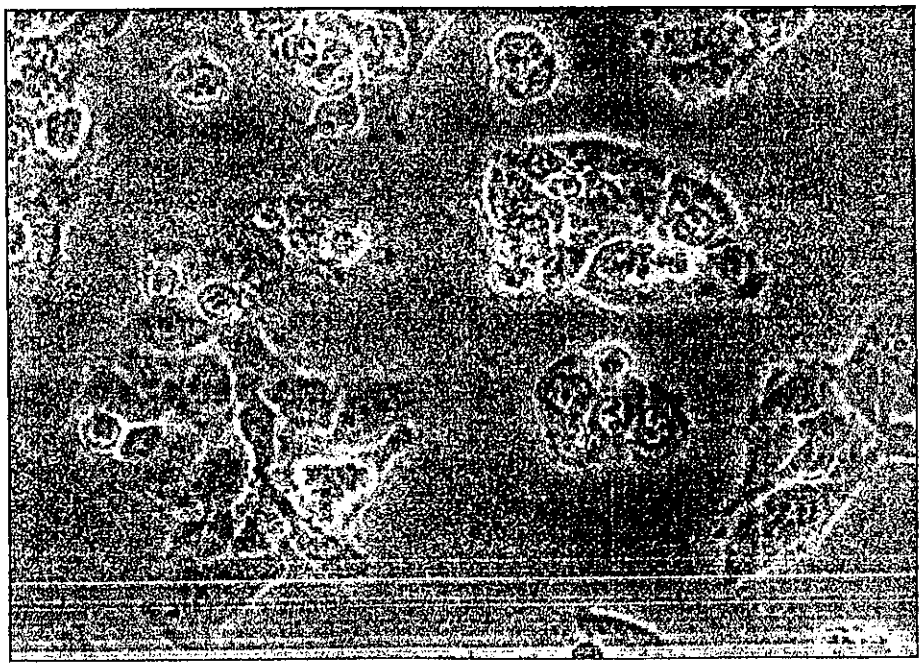

Fig. 1. Cell morphology of E9 cells in culture. HepG2 cells which stably express CYP2E1 (E9 cells) after 24 h treatment with 100 mM ethanol.

hepatozyme (data not shown). For incubation with ethanol, various concentrations of ethanol and other reagents were added to the culture medium. All sample as well as control plates were wrapped with parafilm to minimize evaporation of ethanol. Culture medium and reagents were changed every 24 h. No significant changes in pH were observed in any of the samples.

2.3. Total RNA extraction and quantitative analysis using real-time reverse transcription-PCR

Total RNA from the cell lines was extracted by using RNeasy Mini Kits (QUIAGEN, Valencia, CA) according to the manufacture's protocol.

CTGF mRNA analysis was carried out by the quantitative real-time RT-PCR method; the theoretical base for this method has been described in detail elsewhere [38–40]. Real-time RT-PCR was performed using the ABI PRISM 7700 Sequence Detection System (PE Applied Biosystems, Foster City, CA). The sequence-specific oligonucleotide primers and probe used for CTGF were designed using Primer Express software 1.5 (PE Applied Biosystems, Foster City, CA), as shown below.

CTGF:

Forward 5′-AACCGCAAGATCGGCGT-3′
Reverse 5′-CCGTACCACCGAAGATGCA-3′
Probe 5′-6FAM-TGCACCGCCAAAGATGGTGCTC-TAMRA-3′

Reverse transcription was carried out with 3 mg of total RNA as template using Takara PCR (AMV) kit Ver.2.1 according to the manufacture's protocol (Takara Bio, Shiga, Japan). Each PCR sample contained 5 μl of synthesized cDNA, 12.5 μl of TaqMan 2X Universal Mix (PE Applied Biosystems, Foster City, CA), 2.5 μl of each of the gene-specific probe and primers; water was finally added to the total volume of 25 μl. Primer and TaqMan probe final concentrations in each reaction were 200 and 100 nM, respectively. The actual two-step quantitative PCR was performed as follows: 2 min at 50 °C, 10 min at 95 °C, followed by 40 cycles of 95 °C for 15 s and 60 °C for 1 min.

2.4. Oxidative stress

To verify the presence of protein-bound acrolein, a newly-established potential marker for oxidative stress in the presence or absence of ethanol, anti-acrolein-modified keyhole limpet hemocyanin (KLH) polyclonal antibody or namely mAb5F6, which was kindly provided by Dr. Koji Uchida (Nagoya University, Nagoya, Japan), was used [41,42].

Upon incubation with BSA, acrolein (CH_2=CH–CHO), a ubiquitous pollutant in the environment, was rapidly incorporated into the protein and generated the protein-linked carbonyl derivative, a putative marker of oxidatively modified protein under oxidative stress. The mAb5F6 was raised against the acrolein-modified KLH to verify the protein-bound acrolein in vivo.

The cells were plated on a type I collagen-coated chamber slide (Beckton Dickson, Bedford, MA) at a density of approximately 5×10^3 cells/cm^2 and then adhered on the substratum for 1 h at room temperature. Two hundred microliter hepatozyme, serum-free culture medium, and other reagents as described above were added and the cells were cultured for overnight in the CO_2 incubator at 37 °C. The chamber slide was rinsed three times in phosphate-buffered saline (PBS, pH 7.2) followed by fixation with 4% paraformaldehyde in PBS for 30 min. The chamber slide was then washed twice with PBS, permealized with 0.05% saponin, followed by the incubation with blocking solution (5% sheep serum in PBS) for 60 min. The cells were incubated with the primary antibody, mAb5F6 in 0.1% Triton and 1% BSA for 2 h at room temperature. The chamber slide was washed twice with PBS. The cells were incubated with the secondary antibody (FITC linked anti-mouse IgG made in Sheep) for 1 h (dilute to 1:200 in 1% BSA, 0.1% Triton).

The chamber slide was finally washed twice with PBS. The reacted preparations were examined with a confocal imaging system equipped with a krypton–argon laser (NIKON, Tokyo, Japan).

3. Results

3.1. Connective tissue growth factor (CTGF) mRNA expression in ethanol-treated HepG2 E9 cells constitutively expressing CYP2E1

To evaluate the effect of CYP2E1-mediated ethanol oxidation on CTGF mRNA expression, we used the real-time RT-PCR method for CTGF mRNA quantification. Ethanol is known to be cytotoxic in a dose- and time-dependent manner to E9 cells, which constitutively express CYP2E1 [31–33]. CYP2E1 expression was validated before each experiment by assaying for *p*-nitrophenol oxidation. E9 cells were treated with 100 mM ethanol for 24 and 48 h under serum-free conditions. As shown in Fig. 2, CTGF mRNA levels were significantly higher in ethanol-treated E9 cells at 24 h and further increased at 48 h. In contrast, no substantial increase in CTGF mRNA levels was observed in E9 cells without ethanol treatment (Fig. 2).

Phorbol myristate acetate (PMA), which enhances expression of CYP2E1, has been known to increase cytotoxicity of ethanol to E9 cells. After co-incubation for 24 h with ethanol and PMA, there was nearly a 1.6-fold increase in CTGF mRNA levels (Fig. 3) compared with E9 cells treated with 100 mM ethanol alone. PMA significantly increased CTGF mRNA levels also at 48 h. Since PMA enhanced CYP2E1 expression in E9 cells, this result suggests CYP2E1-mediated ethanol oxidation may be involved in the mechanisms of CTGF upregulation.

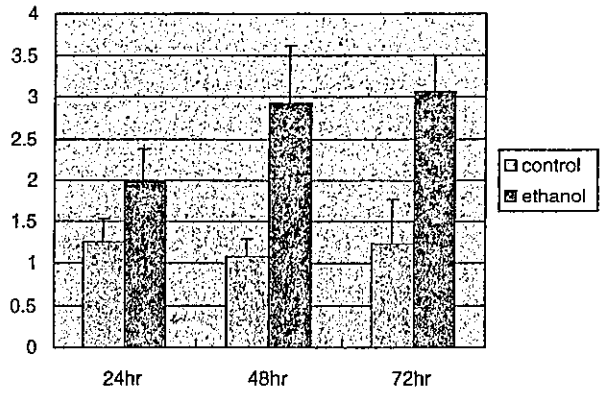

Fig. 2. Time-course effect of ethanol on CTGF mRNA expression in E9 cells. CTGF mRNA was quantified by the real-time RT-PCR method. Results were expressed as threshold cycles (Ct) standardized by Ct for housekeeping gene, GAPDH. CTGF mean mRNA levels of E9 cells ($n = 6$ for 24, 48, 72 h) in the presence or absence of 100 mM ethanol were compared ($n = 6$ for 24, 48, 72 h). At 24 h, CTGF mRNA mean level was significantly higher in ethanol-treated E9 cells than in control cells (1.98 ± 0.40 vs. 1.26 ± 0.26, $P < 0.05$). The same results were observed at 48 h (2.93 ± 0.67 vs. 1.07 ± 0.23, $P < 0.05$) and 72 h (3.05 ± 0.44 vs. 1.23 ± 0.53, $P < 0.05$). Data are expressed as means ± S.D. $P < 0.05$ vs. control.

To further clarify the mechanisms of CTGF upregulation in this cell line model, we used 4-methylpyrazole (4MP), a ligand of CYP2E1. 4MP has been used to be an effective inhibitor of CYP2E1 catalytic activity including oxidation of ethanol. 4MP moderately suppressed CTGF mRNA levels at 24 h after the addition and the significant suppression was attenuated at 48 h (Fig. 4). This result may indicate that inhibition of CYP2E1-mediated ethanol oxidation by 4MP suppressed CTGF mRNA levels.

CTGF mRNA levels in the control cell line were also quantified. MV-5 cells were transfected with only an empty viral vector. These control cells do not stably express detectable CYP2E1. Time-course experiments were carried out

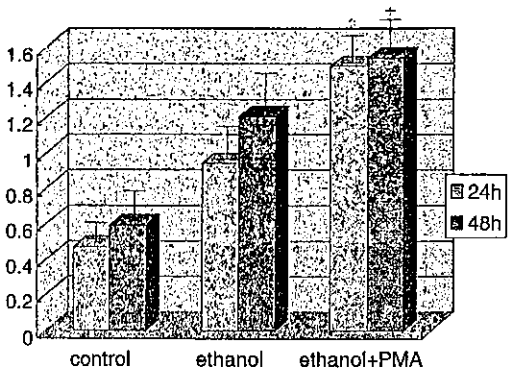

Fig. 3. CYP2E1-dependent Increase of CTGF mRNA Levels. Mean CTGF mRNA levels in E9 control cells ($n = 6$ at 24, 48 h) were compared with E9 cells ($n = 6$ at 24, 48 h) treated with 100 mM ethanol alone, 100 mM ethanol plus Phorbol 12-myrisate 13-acetate (PMA). PMA, a reagent which increases the expression of CYP2E1. PMA significantly enhanced CTGF mRNA expression in ethanol-treated E9 cells. $^{*}P < 0.05$ vs. control. $^{+}P < 0.05$ vs. E9 cells treated with 100 mM ethanol alone.

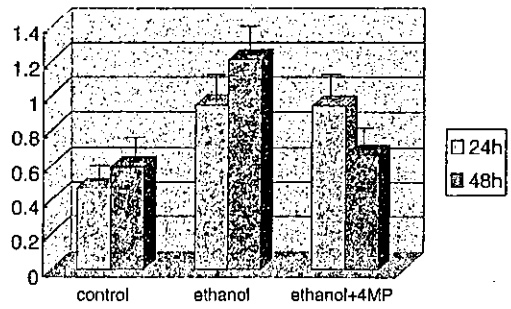

Fig. 4. 4MP, a CYP2E1 inhibitor, reduced CTGF mRNA expression. Mean CTGF mRNA values of ethanol-treated E9 cells ($n = 6$ at 24, 48 h) with and without an addition of 5 mM 4-methylpyrazole (4MP), a ligand of CYP2E1 inhibitor were compared. 4MP has been used to be an effective inhibitor of CYP2E1 catalytic activity including oxidation of ethanol. CTGF mRNA mean level was significantly lower in E9 cells treated with 100 mM ethanol plus 4MP than in E9 cells treated with 100 mM ethanol alone. $^{*}P < 0.05$ vs. control.

to evaluate the effect of ethanol on CTGF mRNA expression. Fig. 5 illustrates that ethanol induced no significant changes in CTGF mRNA levels in MV-5 cells both at 24 and 48 h. Co-incubation with ethanol and PMA induced no significant increase in CTGF mRNA levels in these control cells. Ethanol did not change CTGF mRNA levels in the presence or absence of 4MP in MV-5 cells.

Increased reactive oxygen species production by CYP2E1 metabolism of ethanol may cause CTGF mRNA upregulation in E9 cells. Fig. 6 illustrates the effects of an antioxidant on CTGF mRNA expression. We preincubated E9 cells for 6 h prior to 100 mM ethanol treatment in the presence or absence of *N*-acetylcysteine. Astonishingly, CTGF mRNA levels were reduced by 50% at 24 h and by 80% at 48 h in the presence of *N*-acetylcysteine.

3.2. Visualizing the state of oxidative stress in E9 cells in the absence or presence of ethanol

Various lines of evidence indicate that the ethanol-induced oxidative stress response in the liver plays an important role in the alcoholic liver fibrogenesis. The present study revealed

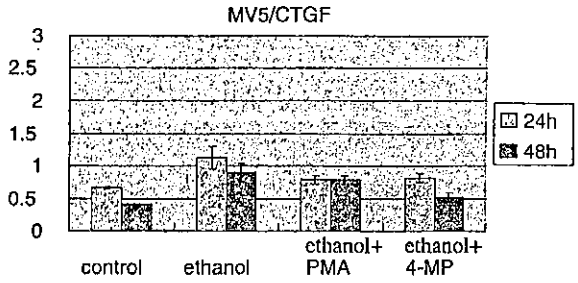

Fig. 5. No CTGF Upregulation in Control Cells. Mean CTGF mRNA levels of MV5 cells ($n = 6$ at 24 and 48 h), which have been transfected with an empty viral vector, were compared. No significant changes in CTGF mRNA levels were observed with (1) 100 mM ethanol ($n = 6$ for 24, 48 h) alone, (2) 100 mM ethanol plus PMA ($n = 6$ for 24, 48 h), or (3) 100 mM ethanol plus 4-MP ($n = 6$ for 24, 48 h).

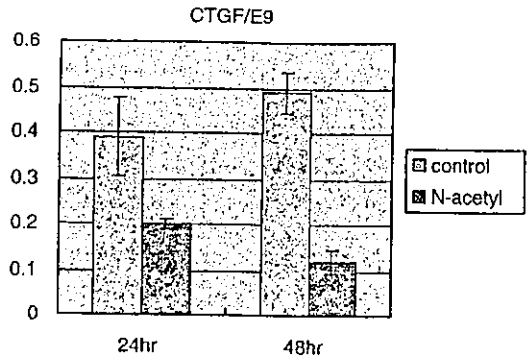

Fig. 6. N-acetylcysteine diminished CTGF Upregulation. Mean CTGF mRNA levels of E9 cells were compared incubated with (1) 100 mM ethanol ($n = 6$ for 24, 48 h) and (2) 100 mM ethanol plus 0.05 mM *N*-acetylcysteine, an inhibitor of lipid peroxidation. CTGF mRNA mean level was significantly lower in E9 cells treated with 100 mM ethanol plus *N*-acetylcysteine compared to control E9 cells treated with 100 mM ethanol alone. $P < 0.05$ vs. control.

CYP2E1 overexpression by PMA upregulated CTGF mRNA and this upregulation was noticeably diminished by an antioxidant. CYP2E1-mediated ethanol oxidation, therefore, is likely to upregulate CTGF mRNA expression.

Ethanol-treated E9 cells were examined histochemically to visualize the state of oxidative stress using anti-acrolein-modified KLH polyclonal antibody, mAb5F6. Since CTGF mRNA quantification in this cell line model was carried out at 24 h after the initial ethanol treatment, we compared E9 cells in the presence or absence of 100 mM ethanol at this time point. Fig. 7 illustrates the result of the immunohistochemical detection of protein-bound acrolein. There was no staining in E9 cells without ethanol treatment (Fig. 7a). E9 cells were stained after treatment for 24 h with 100 mM ethanol (Fig. 7b).

4. Discussion

CTGF is a profibrogenic molecule involved in several human fibrotic disorders including alcoholic hepatic fibrosis. CTGF has attracted much attention as a potential target of future antifibrotic therapies since inhibition of CTGF actions might specifically block profibrotic effects of TGF-β, without affecting anti-proliferative and immunosuppressive effects of TGF-β. Since alcohol is a leading cause of hepatic fibrosis in most Western countries with high morbidity and mortality, the role of CTGF in alcoholic hepatic fibrogenesis should be defined. Our study has first identified a major role of CYP2E1-mediated ethanol oxidation in CTGF gene regulation by using a well-established cell culture model. Indeed, correlation between induction of CYP2E1, lipid peroxidation, and ethanol-induced liver injury has been reported with the continuous intragastric infusion model of ethanol feeding [29,43,44]. Induction of CYP2E1 and the formation of reactive intermediates, such as reactive oxygen species and lipid peroxidation, is one of the central mechanisms by which ethanol becomes hepatotoxic. Our data simply demonstrated that ethanol alone did not upregulate CTGF expression and

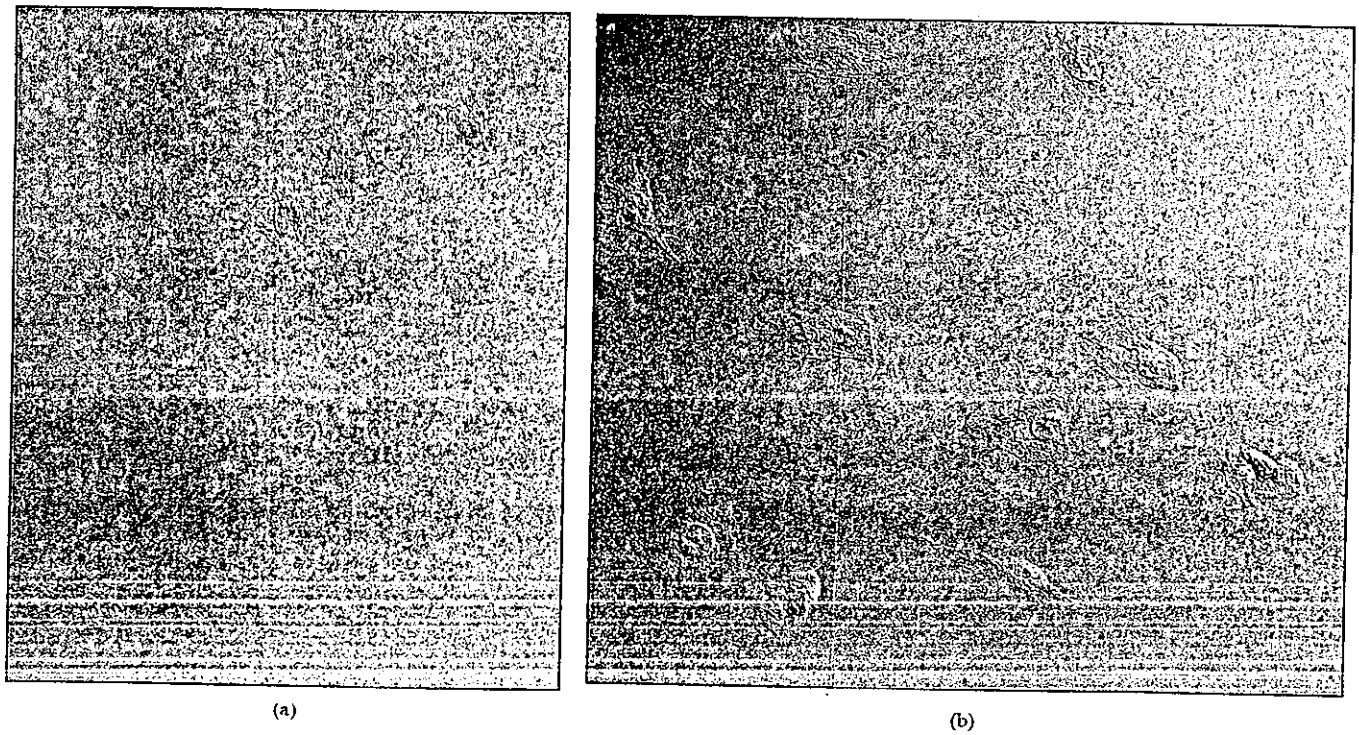

(a) (b)

Fig. 7. Immunohistochemical detection of protein-bound acrolein, a novel marker for oxidative stress. E9 cells untreated (a) and treated with 100 mM ethanol for 24 h (b) were immunostained with anti-acrolein-modified KLH polyclonal antibody, mAb5F6. Only ethanol-treated E9 cells were positive. (original magnification: 200×).

CTGF upregulation seemed to be correlated with and dependent upon the degree of ethanol-inducible CYP2E1 expression. Due to the fact that an antioxidant diminished CTGF upregulation and only ethanol-treated E9 cells were positive for mAb5F6, a putative maker for oxidative stress, CYP2E1-mediated oxidative stress may directly upregulate CTGF expression in alcoholic hepatic fibrogenesis.

Earlier studies on CTGF established a firm relationship between TGF-β actions and CTGF expression [15,18]. TGF-β induces CTGF through different signaling pathways as well as a specific TGF-β responsive element in the CTGF promoter [15]. CTGF may function as a downstream mediator of TGF-β and share some of the fibrogenic actions including the fibroblast proliferation and ECM synthesis [6,15,18,25]. However, exogenous CTGF produced in other cells of the liver and its function to modulate HSC actions has become relevant. Moreover, the existence of TGF-β-independent signaling pathways of CTGF, has also been verified [27]. In our cell culture model, CTGF was produced in transformed hepatocytes, independent of TGF-β actions, since TGF-β was expressed at minimal levels in this cell line even after incubation with 100 mM ethanol (data not shown). Although the relative importance of exogenous CTGF in the activation process of HSCs remains uncertain, CYP2E1-mediated ethanol oxidation may be directly involved in CTGF upregulation in hepatocytes.

The whole regulation processes of liver fibrogenesis, however, are very complex and seem to require activation of signaling pathways of numerous cytokines and growth factors [45]. In ALD, there is a sizable portion of cases with fibrosis without alcoholic hepatitis. A study in the UK [46] has suggested in alcoholic hepatic fibrosis, neither necroinflammation nor an increase in Kupffer cells is an absolute prerequisite for HSC activation and subsequent fibrosis. Since CTGF upregulation in our transformed hapatocytes seems to depend more upon the degree of CYP2E1-mediated ethanol oxidation rather than the degree of inflammation in the liver, it may be concluded that our study provides evidence in part that CTGF is one of the intracellular pro-fibrogenic molecules, mediating activation and proliferation of HSCs in alcoholic hepatic fibrogenesis.

Acknowledgements

The authors thank Dr. Defeng Wu of Mount Sinai School of Medicine for providing technical supports and fruitful discussions.

References

[1] Bradham DM, Igarashi A, Potter RL, Grotendorst GR. Connective tissue growth factor: a cysteine-rich mitogen secreted by human vascular endothelial cells is related to the SRC induced immediate early gene product CEF-10. J Cell Biol 1991;114:1285–94.

[2] Simmons DL, Levy DB, Yannoni Y, Erikson RL. Identification of a phorbol ester-repressible v-src-inducible gene. Proc Natl Acad Sci 1989;86:1178–82.

[3] O'Brien TP, Yang GP, Sanders L, Lay LF. Expression of Cyr 61, a growth factor inducible immediate early gene. Mol Cell Biol 1990;10:3569–77.

[4] Ryseck RP, MacDonald-Bravo H, Mattei MG, Bravo R. Mapping and expression of Fisp-12, a growth factor inducible gene encoding a cystein-rich protein. Cell Growth Differ 1991;2:225–33.

[5] Joliot V, Martinerie C, Dambrine G, Plassiart G, Brisac M, Crochet J, et al. Proviral rearrangements and overexpression of a new cellular gene (nov) in myeloblastosis-associated virus type 1-induced nephroblastomas. Mol Cell Biol 1992;12:10–21.

[6] Paradis V, Dargere D, Vidaud M, De Gouville AC, Huet S, Martinez V, et al. Expression of connective tissue growth factor in experimental and human liver fibrosis. Hepatology 1999;30:968–76.

[7] Igarashi A, Okochi H, Bradham DM, Grotendorst GR. Regulation of connective tissue growth factor gene expression in human skin fibroblasts and during wound repair. Mol Biol Cell 1993;4:637–45.

[8] Lasky JA, Ortiz LA, Tonthat B, Hoyle GW, Corti M, Athas G, et al. Connective tissue growth factor mRNA expression is upregulated in bleomycin-induced lung fibrosis. Am J Physiol 1998;275:L365–71.

[9] Ito Y, Aten J, Bende RJ, Oemar BS, Rabelink TJ, Weening JJ, et al. Expression of connective tissue growth factor in human renal fibrosis. Kidney Int 1998;53:853–61.

[10] Ito Y, Goldschmeding R, Bende RJ, Claessen N, Anwar Chand M, Kleij L, et al. Kinetics of connective tissue growth factor expression during experimental proliferative glomerulonephritis. J Am Soc Nephrol 2001;12:472–84.

[11] di Mola FF, Friess H, Martignoni ME, et al. Connective tissue growth factor is involved in pancreatic repair and tissue remodeling in human and rat acute necrotizing pancreatitis. Ann Surg 2002;235:6–70.

[12] Dammeier J, Brauchle M, Falk W, Grotendorst GR, Werner S. Connective tissue growth factor: a novel regulator of mucosal repair and fibrosis in inflammatory bowel disease? Int J Biochem Cell Biol 1998;30(8):909–22.

[13] Igarashi A, Nashiro K, Kikuchi K, Sato S, Ihn H, Fujimoto M, et al. Connective tissue growth factor gene expression in tissue sections from localized scleroderma, keloid, and other fibrotic skin disorders. J Invest Dermatol 1996;106:729–33.

[14] van Setten GB, Blalock TD, Grotendorst G, Schultz GS. Detection of connective growth factor(CTGF) in human tear fluid: preliminary results. Acta Ophthalmol Scand 2003;81(1):51–3.

[15] Grotendorst GR, Okochi H, Hayashi N. A novel transforming growth factor beta response element controls the expression of the connective tissue growth factor gene. Cell Growth Differ 1996;7:469–80.

[16] Frazier K, Williams S, Kothapalli D, Klapper H, Grotendorst GR. Stimulation of fibroblast cell growth, matrix production, and granulation tissue formation by connective tissue growth factor. J Invest Dermatol 1996;107:404–11.

[17] Kreeva ML, Latinkic BV, Kolesnikova TV, Chen CC, Yang GP, Abler AS, et al. *Cyr*61 and *Fisp*12 are both ECM-associated signaling molecules: activities, metabolism, and localization during development. Exp Cell Res 1997;25:63–77.

[18] Grotendorst GR, Okochi H, Hayashi N. A novel transforming growth factor beta response element controls the expression of the connective tissue growth factor gene. Cell Growth Differ 1996;7:469–80.

[19] Friedman SL, Roll FJ, Boyles, Bissell DM. Hepatic lipocytes: the principal collagen-producing cells of normal rat liver. Proc Natl Acad Sci 1985;82:8681–8685.

[20] Friedman SL. Stellate cell activation in alcoholic fibrosis—an overview. Alcohol Clin Exp Res 1999;23:904–10.

[21] Friedman SL. Molecular regulation of hepatic fibrosis, an integrated cellular response to tissue injury. J Biol Chem 2000;275:2247–50.

[22] Hautekeete ML, Geerts A. The hepatic stellate (Ito) cell: its role in human liver disease. Virchows Arch 1997;430:195–207.

[23] Williams EJ, Arthur MJP, Benyon RC. Increased expression of connective tissue growth factor in fibrotic human liver and activated hepatic stellate cells [Abstract]. Hepatology 1998;28: 300A.
[24] Williams EJ, Gaca MD, Brigstock DR, Arthur MJ, Benyon RC. Increased expression of connective tissue growth factor in fibrotic human liver and in activated hepatic stellate cells. J Hepatol 2000;32: 754–61.
[25] Rachfal AW, Brigstock DR. Connective tissue growth factor (CTGF/CCN2) in hepatic fibrosis. Hepatol Res 2003;26(1):1–9.
[26] Frazier K, Williams S, Kothapalli D, Klapper H, Grotendorst GR. Stimulation of fibroblast cell growth, matrix production, and granulation tissue formation by connective tissue growth factor. J Invest Dermatol 1996;107:404–11.
[27] Paradis V, Perlemuter G, Bonvoust F, Dargere D, Parfait B, Vidaud M, et al. High glucose and hyperinsulinemia stimulate connective tissue growth factor expression: a potential mechanism involved in progression to fibrosis in nonalcoholic steatohepatitis. Hepatology 2001;34:738–44.
[28] Ekstrom G, Ingelman-Sundberg M. Rat liver microsomal NADPH-supported oxidase activity and lipid peroxidation dependent on ethanol-inducible cytochrome P-450 (P-450IIE1). Biochem Pharmacol 1989;38:1313–8.
[29] Tsukamoto H. Oxidative stress, antioxidants, and alcoholic liver fibrogenesis. Alcohol 1993;10:465–7.
[30] Poli G, Parola M. Oxidative damage and fibrogenesis. Free Rad Biol Med 1997;22:287–305.
[31] Kamimura S, Gaal K, Britton RS, Bacon BR, Triadafilopoulos G, Tsukamoto H. Increased 4-hydroxynonenal levels in experimental alcoholic liver disease: association of lipid peroxidation with liver fibrogenesis. Hepatology 1992;16:448–53.
[32] Oinonen T, Koivisto T, Lindros KO. No significant expression of CYP2E1 in rat stellate cells. Biochem Pharmacol 1998;56(8): 1075–8.
[33] Casini A, Pellegrini G, Ceni E, Salzano R, Parola M, Robino G, et al. Human hepatic stellate cells express class I alcohol dehydrogenase and aldehyde dehydrogenase but not cytochrome P4502E1. J Hepatol 1998;28(1):40–5.
[34] Wu D, Cederbaum AI. Ethanol-induced apoptosis to stable HepG2 cell line expressing cytochrome P-4502E1. Alcohol Clin Exp Res 1999;23(1):67–76.
[35] Mari M, Wu D, Nieto N, Cederbaum AI. CYP2E1-dependent toxicity and up-regulation of antioxidant genes. J Biomed Sci 2001;8:52–8.
[36] Wu D, Cederbaum AI. Ethanol cytotoxicity to a transfected HepG2 cell line expressing human cytochrome P4502E1. J Biol Chem 1996;271:23914–9.
[37] Chen Q, Galleano M, Cederbaum AI. Cytotoxicity and apoptosis produced by arachidonic acid in HepG2 cells overexpressing human cytochrome P4502E1. J Biol Chem 1997;272:14532–41.
[38] Heid CA, Stevens J, Livak KJ, Williams PM. Real time quantitative PCR. Genome Res 1996;6:986–94.
[39] Gibson UEM, Heid CA, Willaims PM. A novel method for real time quantitative RT-PCR. Genome Res 1996;6:995–1000.
[40] Bieche I, Laurendeau I, Tozlu S, Olivi M, Vidaud D, Lidereau R, et al. Quantitation of myc gene expression in sporadic breast tumors with a real-time reverse transcription-PCR assay. Cancer Res 1999;59: 2759–65.
[41] Uchida K, Kanematsu M, Sakai K, Matsuda T, Hattori N, Mizuno Y, et al. Protein-bound acrolein: potential markers for oxidative stress. Proc Natl Acad Sci 1998;95:4882–7.
[42] Uchida K, Kanematsu M, Morimitsu Y, Osawa T, Noguchi N, Niki N. Acrolein is a product of lipid peroxidation reaction. Formation of free acrolein and its conjugate with lysine residues in oxidized low-density lipoproteins. J Biol Chem 1998;273:16058–66.
[43] Morimoto M, Hagbjork AL, Nanji AA, et al. Role of cytochorome P45022E1 in alcoholic liver disease pathogenesis. Alcohol 1993;10(6):459–64.
[44] French SW. Biochemistry of alcoholic liver disease. Crit Rev Clin Lab Sci 1992;29(2):83–115.
[45] Chenn MM, Lam A, Abraham JA, Schreiner GF, Joly AH. CTGF expression is induced by TGF-β in cardiac fibroblasts and cardiac myocytes: a potential role in heart fibrosis. J Mol Cell Cardiol 2000;32:1805–19.
[46] Reeves HL, Burt AD, Wood S, Day CP. Hepatic stellate cell activation occurs in the absence of hepatitis in alcoholic liver disease and correlates with the severity of steatosis. J Hepatol 1996;25:677–83.

Am J Physiol Gastrointest Liver Physiol 287: G695–G705, 2004.
First published March 25, 2004; 10.1152/ajpgi.00415.2003.

Bax interacts with the voltage-dependent anion channel and mediates ethanol-induced apoptosis in rat hepatocytes

Masayuki Adachi,[1] Hajime Higuchi,[1] Soichiro Miura,[2] Toshifumi Azuma,[1] Sayaka Inokuchi,[1] Hidetsugu Saito,[1] Shinzo Kato,[1] and Hiromasa Ishii[1]

[1]*Department of Internal Medicine, Keio University School of Medicine, Shinjuku-ku, Tokyo, 160-8582; and* [2]*Second Department of Internal Medicine, National Defense Medical College, Tokorozawa, Saitama, 359-8513, Japan*

Submitted 24 September 2003; accepted in final form 22 March 2004

Adachi, Masayuki, Hajime Higuchi, Soichiro Miura, Toshifumi Azuma, Sayaka Inokuchi, Hidetsugu Saito, Shinzo Kato, and Hiromasa Ishii. Bax interacts with the voltage-dependent anion channel and mediates ethanol-induced apoptosis in rat hepatocytes. *Am J Physiol Gastrointest Liver Physiol* 287: G695–G705, 2004. First published March 25, 2004; 10.1152/ajpgi.00415.2003.—Acute ethanol exposure induces oxidative stress and apoptosis in primary rat hepatocytes. Previous data indicate that the mitochondrial permeability transition (MPT) is essential for ethanol-induced apoptosis. However, the mechanism by which ethanol induces the MPT remains unclear. In this study, we investigated the role of Bax, a proapoptotic Bcl-2 family protein, in acute ethanol-induced hepatocyte apoptosis. We found that Bax translocates from the cytosol to mitochondria before mitochondrial cytochrome *c* release. Bax translocation was oxidative stress dependent. Mitochondrial Bax formed a protein complex with the mitochondrial voltage-dependent anion channel (VDAC). Prevention of Bax-VDAC interactions by a microinjection of anti-VDAC antibody effectively prevented hepatocyte apoptosis by ethanol. In conclusion, these data suggest that Bax translocation from the cytosol to mitochondria leads to the subsequent formation of a Bax-VDAC complex that plays a crucial role in acute ethanol-induced hepatocyte apoptosis.

alcoholic liver disease; mitochondria; oxidative stress; cytochrome *c*

HEPATOCYTE APOPTOSIS IS RECOGNIZED in the liver of both clinical (19, 30) and experimental (2, 9) alcohol-related injury and is currently identified as a common feature of alcoholic liver disease. Although both oxidative stress and cytokines, i.e., TNF-α or transforming growth factor-β, have been suggested as crucial mediators of hepatocyte apoptosis in alcoholic liver disease (15, 18, 28), relatively little is known regarding the intracellular mechanisms by which ethanol induces hepatocyte apoptosis. Our previous studies demonstrated that short-term ethanol intoxication causes oxidative stress, mitochondrial dysfunction (21), and apoptosis (12, 22) in primary cultured rat hepatocytes. In these studies, ethanol induced oxidative stress by an alcohol dehydrogenase-dependent mechanism (21) and was associated with loss of the mitochondrial membrane potential ($\Delta\psi$). This loss of $\Delta\psi$ signified a change in the mitochondrial inner membrane permeability (22) and was associated with cytochrome *c* release into the cytosol (12). Cytochrome *c* may bind to apoptosis-activating factor-1 and procaspase-9, resulting in activation of caspase-9, followed by activation of effector caspase-3, -6, and -7 (34, 39). Indeed, we observed both caspase-3 and -9 activation in ethanol-treated hepatocytes, whereas activation of caspase-8 or Bid was not detected (12). Thus mitochondrial dysfunction, such as cytochrome *c* release, may initiate ethanol-induced hepatocyte apoptosis. However, the exact mechanisms responsible for the cytochrome *c* release by acute ethanol cytotoxicity are unclear.

Permeability of the inner mitochondrial membrane is regulated by the permeability transition pore (PTP) (3, 42). The exact nature of the PTP remains in dispute. One model suggests that the PTP is comprised of the outer membrane protein voltage-dependent anion channel (VDAC), the inner membrane protein adenine nucleotide translocator (ANT), and cyclophillin-D at outer and inner membrane contact sites (4). Although opening of the PTP is transient and does not cause swelling (14, 32), sustained opening of the PTP might cause mitochondrial swelling with secondary rupture of the outer membrane (31). This rupture of outer membrane leads to massive cytochrome *c* release that has been noted in both apoptotic and necrotic cell death (24). We previously reported (3) that ethanol-induced cytochrome *c* release and apoptosis were blocked by cyclosporin A (CsA), an inhibitor of the PTP component cylophillin-D, suggesting that ethanol-induced cytochrome *c* release is PTP dependent. However, the mechanism by which ethanol induces the PTP opening remains to be elucidated. Recently, the role of proapoptotic Bcl-2 family proteins in mediating the mitochondrial permeability pore has been suggested (10, 38). Therefore, we hypothesized that Bcl-2-related proteins may contribute to cytochrome *c* release during alcohol cytotoxicity.

Bax and Bak, proapoptotic members of the Bcl-2 family, are crucial for apoptosis (8). Bax translocates from the cytosol to the mitochondrial outer membrane in many models of apoptosis (7). Bax inserts into the mitochondrial outer membrane on apoptotic stimuli (13, 40). Bax homotypic complex or heterotypic complex with Bak promote cytochrome *c* release from the intermembrane space of mitochondria into the cytosol (17). An in vitro study has shown that treatment of liposomes with Bax permeabilizes lipid membranes, allowing translocation of cytochrome *c* from the liposomes into the media and suggesting homotypic oligomerized channel formation composed of at least four Bax molecules (33). On the other hand, heterotypic interactions of Bax with the PTP components VDAC (29) or ANT (25) have also been suggested. Therefore, Bax may regulate VDAC or ANT function via direct molecular interactions. Interestingly, Bax-VDAC heterotypic interactions can form a large pore that is permeable to cytochrome *c* (35). The

Address for reprint requests and other correspondence: H. Ishii, Dept. of Internal Medicine, School of Medicine, Keio Univ., 35 Shinanomachi, Shinjuku-ku, Tokyo, 160-8582, Japan.

The costs of publication of this article were defrayed in part by the payment of page charges. The article must therefore be hereby marked "*advertisement*" in accordance with 18 U.S.C. Section 1734 solely to indicate this fact.